NREL Pyrheliometer Comparisons: September 25 – October 1, 2022 (NPC-2022)

Ibrahim Reda, Afshin Andreas, Martina Stoddard, Mark Kutchenreiter, and Aron Habte

National Renewable Energy Laboratory

NREL is a national laboratory of the U.S. Department of Energy
Office of Energy Efficiency & Renewable Energy
Operated by the Alliance for Sustainable Energy, LLC

This report is available at no cost from the National Renewable Energy Laboratory (NREL) at www.nrel.gov/publications.

Contract No. DE-AC36-08GO28308

Technical Report
NREL/TP-1900-84219
November 2022

NREL Pyrheliometer Comparisons: September 25 – October 1, 2022 (NPC-2022)

Ibrahim Reda, Afshin Andreas, Martina Stoddard, Mark Kutchenreiter, and Aron Habte

National Renewable Energy Laboratory

Suggested Citation
Reda, Ibrahim, Afshin Andreas, Martina Stoddard, Mark Kutchenreiter, Aron Habte. 2022. *NREL Pyrheliometer Comparisons: September 25 – October 1, 2022 (NPC-2022).* Golden, CO: National Renewable Energy Laboratory. NREL/TP-1900-84219. https://www.nrel.gov/docs/fy23osti/84219.pdf.

NREL is a national laboratory of the U.S. Department of Energy
Office of Energy Efficiency & Renewable Energy
Operated by the Alliance for Sustainable Energy, LLC

This report is available at no cost from the National Renewable Energy Laboratory (NREL) at www.nrel.gov/publications.

Contract No. DE-AC36-08GO28308

Technical Report
NREL/TP-1900-84219
November 2022

National Renewable Energy Laboratory
15013 Denver West Parkway
Golden, CO 80401
303-275-3000 • www.nrel.gov

NOTICE

This work was authored by the National Renewable Energy Laboratory, operated by Alliance for Sustainable Energy, LLC, for the U.S. Department of Energy (DOE) under Contract No. DE-AC36-08GO28308. Funding provided by U.S. Department of Energy Office of Energy Efficiency and Renewable Energy Solar Energy Technologies Office. The views expressed herein do not necessarily represent the views of the DOE or the U.S. Government.

This report is available at no cost from the National Renewable Energy Laboratory (NREL) at www.nrel.gov/publications.

U.S. Department of Energy (DOE) reports produced after 1991 and a growing number of pre-1991 documents are available free via www.OSTI.gov.

Cover Photos by Dennis Schroeder: (clockwise, left to right) NREL 51934, NREL 45897, NREL 42160, NREL 45891, NREL 48097, NREL 46526.

NREL prints on paper that contains recycled content.

Acknowledgments

We sincerely appreciate the support of Solar Radiance Research Laboratory (SRRL) staff and National Renewable Energy Laboratory (NREL) management, the U.S. Department of Energy (DOE) Office of Energy Efficiency and Renewable Energy Solar Energy Technologies Program, the DOE Environmental Research/Atmospheric Radiation Measurement Program, and NREL's Environment, Safety, Health, & Quality center. Our thanks also go to all the participants for their patience and cooperation during NREL Pyrheliometer Comparisons 2022, a weather-dependent exercise.

NPC-2022 participants, by Joe DelNero

List of Acronyms and Abbreviations

AEMET	State Meteorological Agency (Spain)
AHF	Automatic Hickey-Frieden
BMS	Baseline Measurement System
BORCAL	Broadband Outdoor Radiometer Calibration
DOE	U.S. Department of Energy
IPC	International Pyrheliometer Comparison
IPC-XIII	Thirteenth International Pyrheliometer Comparisons
ISO	International Organization for Standardization
MST	Mountain Standard Time
NOAA/ESRL/GMD	National Oceanic and Atmospheric Administration's Earth System Research Laboratory, Global Monitoring Division
NPC	NREL Pyrheliometer Comparisons
NREL	National Renewable Energy Laboratory
PMOD/WRC	Physikalisch-Meteorologisches Observatorium Davos—World Radiation Center
SDp	pooled standard deviation
SI	International System of Units
SRRL	Solar Radiation Research Laboratory
TSG	Transfer Standard Group
WMO	World Meteorological Organization
WRR	World Radiometric Reference
WRR-TF	World Radiometric Reference transfer factor
WSG	World Standard Group
%uA	Percentage Type-A standard uncertainty
NRdg	number of readings
uC	combined standard uncertainty
Eff DF	effective degrees of freedom

Executive Summary

Accurate measurements of direct normal (beam) solar irradiance from pyrheliometers[1] are important for developing and deploying solar energy conversion systems, for improving our understanding of Earth's energy budget for climate change studies, and for other science and technology applications involving solar flux. Providing these measurements places many demands on the quality system used by the operator of commercially available radiometers. Maintaining accurate radiometer calibrations that are traceable to an international standard is the first step in producing research-quality solar irradiance measurements.

In 1977, the World Meteorological Organization (WMO) established the World Radiometric Reference (WRR) as the international standard for the measurement of direct normal solar irradiance (Fröhlich 1991). The WRR is an internationally recognized, detector-based measurement standard determined by the collective performance of six electrically self-calibrated absolute cavity radiometers comprising the World Standard Group (WSG). Various countries, including the United States,[2] have contributed these specialized radiometers to the Physikalisch-Meteorologisches Observatorium Davos—World Radiation Center (PMOD/WRC) to establish the WSG.

As with all measurement systems, Absolute Cavity Radiometers (ACR) are subject to performance changes over time. Therefore, PMOD/WRC in Davos, Switzerland, hosts an quinquennial International Pyrheliometer Comparison (IPC) event for transferring the WRR to participating radiometers by invitation.[3] The National Renewable Energy Laboratory (NREL) has represented the U.S. Department of Energy (DOE) in each IPC since 1980. And NREL has developed and maintained a select group of absolute cavity radiometers with direct calibration traceability to the WRR, and it uses these reference instruments to calibrate pyrheliometers and pyranometers using the International Organization for Standardization (ISO) 17025-accredited Broadband Outdoor Radiometer Calibration (BORCAL) process (Reda et al. 2008).

To fill the gap between each IPC, NREL pyrheliometer comparisons (NPCs) are held annually at the Solar Radiation Research Laboratory (SRRL) in Golden, Colorado. Open to all ACR owners and operators, each NPC provides an opportunity to determine the unique WRR transfer factor (WRR-TF) for each participating pyrheliometer. By adjusting all subsequent pyrheliometer measurements by the appropriate WRR-TF, the solar irradiance data are traceable to the WRR.

NPC-2022 was held September 25 through October 1, 2022. Participants operated 42 ACRs to simultaneously measure clear-sky direct normal solar irradiance during this period. The Transfer Standard Group (TSG) of reference radiometers for NPC-2022 consisted of four NREL radiometers with direct traceability to the WRR, each having participated in the Thirteenth International Pyrheliometer Comparisons (IPC-XIII) in the fall of 2021 (delayed one year due to COVID-19). As a result of NPC-2022, each participating absolute cavity radiometer was

[1] Pyrheliometers are a type of radiometer used to measure solar irradiance (i.e., radiant flux in Watts per square meter) on a surface normal to the apparent solar disk within a 5.0° or 5.7° field of view, depending on the optical design of the instrument. A solar tracker is used to maintain proper alignment of the pyrheliometer with the sun during daylight periods.

[2] The WSG includes radiometers on permanent loan from the Eppley Laboratory, Inc., and NREL.

[3] Appendix A lists the NPC-2022 participants and the pyrheliometers compared.

assigned a new WRR-TF, which is computed as the reference irradiance determined by the TSG divided by the observed irradiance from the participating radiometer. The performance of the TSG during NPC-2022 was consistent with previous comparisons, including IPC-XIII. The measurement performance of the TSG allowed the transfer of the WRR to each participating radiometer with an estimated uncertainty of ± 0.33% with respect to the International System of Units.

The comparison protocol is based on data collection periods called *runs*. Each measurement run consists of an electrical self-calibration requiring five minutes for the Automatic Hickey-Frieden (AHF) cavities, a series of 49 solar irradiance measurements at 30-second intervals, and a post-calibration. more than 2000 reference irradiance measurements during NPC-2022. The clear-sky daily maximum direct normal irradiance level was 1,003 Wm^{-2}.

Ancillary environmental conditions (e.g., broadband turbidity, ambient temperature, relative humidity, wind speed, precipitable water vapor, and spectral data) collected at SRRL during the comparison are presented in Appendix B to document the environmental test conditions.

NPCs are planned annually at the SRRL to ensure worldwide homogeneity of solar radiation measurements traceable to the WRR.

Table of Contents

List of Figures

List of Tables

1 Introduction

Accurate measurements of broadband solar irradiance require radiometers with proper design and performance characteristics, correct installation, and documented operation and maintenance procedures, including regular calibration. Calibrations of any measuring device must be traceable to a recognized reference standard. The World Radiometric Reference (WRR) is the internationally recognized measurement standard for direct normal irradiance measurements of broadband solar radiation (Fröhlich 1991).

The WRR was established by the World Meteorological Organization (WMO) in 1977 and has been maintained by the Physikalisch-Meteorologisches Observatorium Davos—World Radiation Center (PMOD/WRC)[4] in Switzerland. The WRR is maintained for broadband solar irradiance with an absolute uncertainty of better than ± 0.3% with respect to the International System of Units (SI) (Romero et al. 1996). The WRR standard is widely used to calibrate pyrheliometers and pyranometers with a wavelength response range that is compatible with the solar spectrum wavelengths of 280–3,000 nm.

Every five years, the WRR is transferred to WMO regional centers and other participants at the International Pyrheliometer Comparisons (IPC) event, which is held at the PMOD/WRC. The Thirteenth IPC (IPC-XIII) was completed in 2021 (Finsterle 2022). At each IPC, instantaneous measurements from the World Standard Group (WSG) are compared at 90-second intervals with the data from participating radiometers recorded under clear-sky conditions. A new WRR transfer factor (WRR-TF) is calculated for each participating radiometer based on the mean WRR of the WSG radiometers for each IPC. Multiplying the irradiance reading of each radiometer by its assigned WRR-TF will result in measurements that are traceable to SI units through the WRR and are therefore consistent with the international reference of solar radiation measurement.

In compliance with International Organization for Standardization (ISO) 17025 accreditation requirements for demonstrating interlaboratory proficiency, the National Renewable Energy Laboratory (NREL) hosts annual pyrheliometer comparisons at the Solar Radiation Research Laboratory (SRRL) in Golden, Colorado, for non-IPC years. The NREL Pyrheliometer Comparisons in 2022 (NPC-2022) was September 25 through October 1, 2022, at the SRRL. Participants operated absolute cavity radiometers during the comparisons. See Appendix A for a list of participants and affiliations.

The results presented in this report are based on clear-sky, direct normal solar irradiance data collected during NPC-2022. See Appendix B for the environmental conditions during NPC-2022.

[4] https://www.pmodwrc.ch

2 Reference Instruments

NREL developed the transfer standard group (TSG) of four Absolute Cavity Radiometers (ACR) to serve as the transfer reference for each NPC. The radiometers comprising the TSG were included in the most recent IPC and maintain the WRR for NREL (see Table 1). Using the method described by Reda (1996), the mean of the TSG measurements was maintained for establishing the reference irradiance data for NPC-2022 data reduction. Table 1 lists the TSG absolute cavity radiometers with their WRR-TFs and pooled standard deviation (SD_p) as determined from the latest IPC in 2021 (Finsterle 2022).

Table 1. Summary of IPC-XIII Results for the NPC-2022 TSG

Serial Number	WRR Factor (IPC-XIII)	Standard Deviation (%)	Number of Readings
AHF28968	0.99802	0.0714	1066
AHF29220	0.99779	0.0696	1060
AHF30713	0.99760	0.0668	1058
TMI68018	0.99685	0.0738	1108
Mean WRR for the TSG	0.99756	**SDp for the TSG:** 0.0705%	

The pooled standard deviation, SD_p , for the TSG was computed from the following equation:

$$SD_p = \sqrt{\frac{\sum_{i=1}^{m} n_i * S_i^2}{\sum_{i=1}^{m} n_i}} \qquad 1$$

where:

- i = i^{th} cavity
- m = number of reference cavities
- Si = standard deviation of the ith cavity, from IPC-XIII
- n_i = number of readings of the ith cavity, from IPC-XIII.

3 Measurement Protocol

The decision to deploy instruments for a comparison was made daily during NPC-2022. Data were collected only during clear-sky conditions, which were determined visually and from the stability of pyrheliometer readings. Simultaneous direct normal solar irradiance measurements were taken by most cavity radiometers in groups of 49 observations at 30-second intervals (PMO6 and PMO8 used 120-, 90-, 60-, or 30-second open/closed-shutter cycles).

Each group of observations is called a *run*. An electrical self-calibration of each Automatic Hickey-Frieden (AHF) ACR was performed before each run. Previous WRR-TFs determined from results of IPCs or NPCs were *not* applied to the observations. The original manufacturer's calibration factor was used according to the standard operating procedure provided by the manufacturer for each radiometer. A timekeeper announced the beginning of each calibration period and gave a six-minute countdown before the start of each run to facilitate the AHF cavity self-calibrations and the simultaneous start for each participant.

By consensus, at least 300 observations from each radiometer were required to determine the WRR-TF for an NPC. A statistically significant data set was required to derive the WRR-TF for each pyrheliometer. Data from each pyrheliometer/operator system were emailed at the end of the day.

4 Transferring of the World Radiometric Reference

The primary purpose of an NPC is to transfer the current WRR from the NPC-TSG to each participating ACR. This requires that the participating pyrheliometers and the TSG collect simultaneous measurements of clear-sky direct normal (beam) solar irradiance.

4.1 Calibration Requirements

Following WMO guidelines (Romero 1995), the following conditions were required before data collection was accomplished during NPC-2022:

- The radiation source was the sun, and irradiance levels were > 700 Wm^{-2}.
- A Digital Multimeter with an uncertainty < 0.05% or better was used to measure the thermopile signals from each radiometer.
- Solar trackers were aligned with a slope angle within ± 0.25°.
- Wind speed was low (< 5 m/s) from the direction of the solar azimuth ± 30°.
- Cloud cover was < 1/8 of the sky dome, with an angular distance > 15° from the sun.

4.2 Determining the Reference Irradiance

Four ACRs that are maintained by NREL and were part of IPC-XIII were used as the TSG to transfer the WRR in the comparison. The WRR-TF for each TSG is presented in Table 1 (above). The reference irradiance at each reading was calculated using the following steps, as described by Reda (1996):

1. Each irradiance reading of the TSG is divided by the irradiance measured by AHF 28968, for its participation in many IPCs.
2. By maintaining the mean of WRR for the TSG, a new WRR-TF for NPC-2022 is recalculated for each of the TSG cavities (see Figure 1).
3. The reference irradiance for each 30-second observation in a run is computed as the mean of the simultaneous reference irradiances measured by the TSG. The reference irradiance reading for each cavity in the TSG is the irradiance reading of the cavity multiplied by its new WRR-TF calculated in Step 2.

4.3 Data Analysis Criteria

AHF 28968 was used to check irradiance stability at the time of each comparison reading during a run. Stable irradiance readings are defined to within 1.0 Wm^{-2} during an interval of two seconds centered on each reading time (i.e., one second before and one second after the recorded reading). Unstable irradiance readings were marked in the data record and automatically rejected from the data analysis; historically, this has affected fewer than 10% of the data collected during an NPC. Also rejected were all calculated ratios of the test instrument irradiance divided by AHF 28968 irradiance that deviated from their mean by 0.3% (Reda 1996). Typically, data rejected from the analysis in this manner were the result of failed tracker alignment, problems with the pre-calibration, or a similar cause for bias greater than expected from a properly functioning absolute cavity radiometer.

4.4 Measurements

NPC-2022 was completed for all participants on October 1, after more than 2000 data points were collected by the reference cavities during the requisite clear-sky conditions. The actual number of readings for each participating radiometer compared with the reference irradiance varied according to the data analysis selection criteria described above.

4.5 Results

The historical results for the TSG are presented in Figure 1. To evaluate the performance of these instruments, the standard deviations of each radiometer were monitored during the comparisons. The results suggest successful performance of the TSG during this NPC.

For the TSG, the NPC-2022 WRR-TF did not change by more than a fraction of the standard deviation derived during IPC-XIII in 2021 (see Figure 1. History of WRR reduction factors for NREL reference cavities).

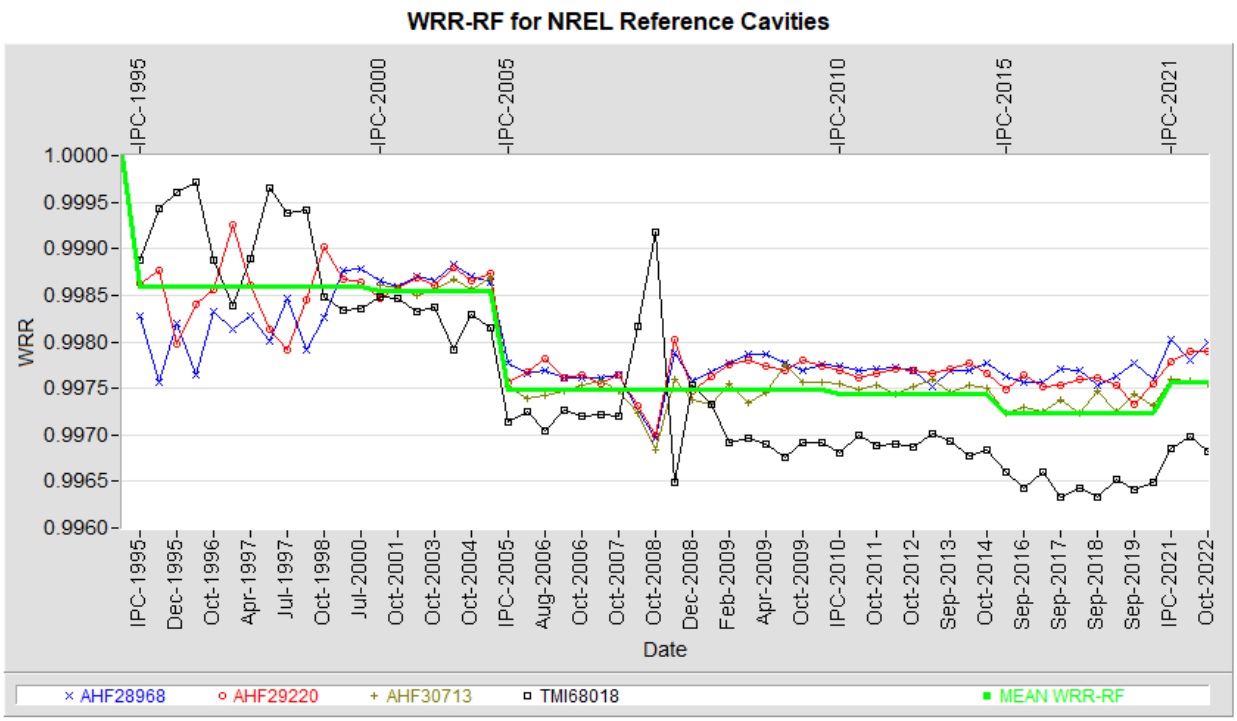

Figure 1. History of WRR reduction factors for NREL reference cavities. Note that in 2008, a spider web was discovered in TMI68018.

For NPC-2022 Proficiency Test, the results of the participating cavities in IPC-XIII and NPC-2022 were evaluated using the following equation:

$$E_n = \frac{WRR_{NPC} - WRR_{IPC}}{\sqrt{U95^2_{NPC} + U95^2_{IPC}}} \qquad 2$$

where E_n must lie in the interval -1 to +1.

From Table 2, E_n for all cavities was well within the interval -1 to +1 (i.e., the WRR from NPC-2022 is consistent with the WRR from IPC-XIII).

Results for each radiometer participating in NPC-2022 are presented in Table 3.

Table 2. Summary of Results for Proficiency Test During NPC-2022

Participating Cavity	NPC-2022 WRR	%U95	IPC WRR	%U95	IPC Year	En
AHF14915	0.99982	0.42	0.99983	0.36	2021	-0.00
AHF23734	0.99851	0.38	0.99867	0.34	2021	-0.03
AHF27798	0.99999	0.38	1.00100	0.50	2021	-0.16
AHF28553	0.99791	0.38	0.99774	0.35	2015	0.03
AHF28560	1.00057	0.38	1.00030	0.37	2021	0.05
AHF30110	1.07747	0.40	1.07222	1.38	2021	0.34
AHF31041	0.99805	0.39	0.99639	0.36	2015	0.31
AHF31105	0.99843	0.39	0.99866	0.36	2015	-0.04
AHF32455	1.00147	0.40	1.00147	0.34	2021	0.00
AHF34926	1.00159	0.39	1.00136	0.34	2021	0.04
AHF37816	0.99956	0.38	0.99952	0.34	2021	0.01
PMO6 0401	1.02165	0.40	1.02165	0.33	2021	-0.00
PMO6 0803	1.00045	0.40	1.00029	0.32	2021	0.03
PMO6 0816	0.99935	0.42	0.99919	0.39	2021	0.03
PMO6 5	0.99963	0.39	0.99956	0.35	2021	0.01
PMO8 F201007A	1.00606	0.40	1.00633	0.33	2021	-0.05

Table 3. Summary of Results for Radiometers Participating in NPC-2022

Cavity	WRR (NPC-2022)	SD	NRDG	%U95
AHF14915	0.99982	0.0010	1257	0.42
AHF14917	0.99847	0.0005	1328	0.38
AHF17142	0.99867	0.0006	1662	0.38
AHF23734	0.99851	0.0004	2384	0.38
AHF27798	0.99999	0.0005	1537	0.38
AHF28553	0.99791	0.0005	1328	0.38
AHF28556	0.99226	0.0011	1645	0.43
AHF28560	1.00057	0.0006	1507	0.38
AHF29219	1.06310	0.0008	2328	0.39
AHF29222	1.05913	0.0007	1658	0.39
AHF30110	1.07747	0.0009	327	0.40
AHF30495	1.05561	0.0009	1659	0.41
AHF31041	0.99805	0.0007	1208	0.39
AHF31102	1.00129	0.0006	1402	0.39
AHF31104	1.03884	0.0012	2414	0.44
AHF31105	0.99843	0.0007	1218	0.39
AHF31108	0.99808	0.0006	1687	0.39
AHF31109	0.99806	0.0007	1468	0.39
AHF32452	1.03144	0.0009	2290	0.40
AHF32455	1.00147	0.0008	414	0.40
AHF34926	1.00159	0.0006	1241	0.39
AHF36767	0.99797	0.0009	1091	0.40
AHF37816	0.99956	0.0005	1400	0.38
AHF37817	1.00023	0.0013	1273	0.45
AWX31114	1.00172	0.0008	1350	0.40
AWX31116	1.06999	0.0011	1294	0.42
AWX32448	1.00070	0.0005	1350	0.38
CHP1 120994	0.99044	0.0020	2390	0.53
NIP 9013	1.00641	0.0051	2206	1.05
PMO6 0401	1.02165	0.0009	405	0.40
PMO6 0803	1.00045	0.0008	<300	0.40
PMO6 0816	0.99935	0.0011	425	0.42
PMO6 1601	1.00355	0.0006	391	0.38
PMO6 5	0.99963	0.0007	1101	0.39
PMO6 850404	1.00090	0.0007	1424	0.39
PMO8 F201007A	1.00606	0.0009	366	0.40
PMO8 F211004	0.99965	0.0008	520	0.40
PMO8 F211007	0.99955	0.0008	514	0.40
TMI67603	1.00004	0.0006	1690	0.39
TMI67811	0.99986	0.0010	1599	0.41
TMI67916	0.99946	0.0008	1708	0.40
TMI68022	1.00021	0.0012	1688	0.43

The uncertainty of the WRR-TF associated with each participating radiometer with respect to SI was calculated using the following equation:

$$U_{95} = \pm 1.96 * \sqrt{u_A^2 + u_B^2} \qquad 3$$

where:

- U95 = uncertainty of the WRR-TF (in percent) determined at NPC-2022 with 95% confidence level
- 1.96 = coverage factor
- uA = Type A standard uncertainty = standard deviation of each participating radiometer (in %) determined at NPC-2022
- uB = Type B standard uncertainty
- uB = $\pm \sqrt{(\frac{0.3}{\sqrt{3}})^2 + 0.0705^2}$

  where:

  - 0.3 = Estimated expanded uncertainty of the WRR scale with respect to SI, in %
  - $\sqrt{3}$ = Coverage factor for rectangular distribution
  - 0.0705 = Pooled standard deviation of the four reference radiometers (TSG) that participated in IPC-XIII (September/October 2021), in %.

The statistical analyses of WRR-TF for the participating pyrheliometers are presented in Figure 2 through Figure 7. These graphical summaries indicate the mean, standard deviation, and histograms of the WRR-TF determined during NPC-2022. If the participating pyrheliometer has a known WRR from a previous year, the percentage change in the WRR is listed in Table 4.

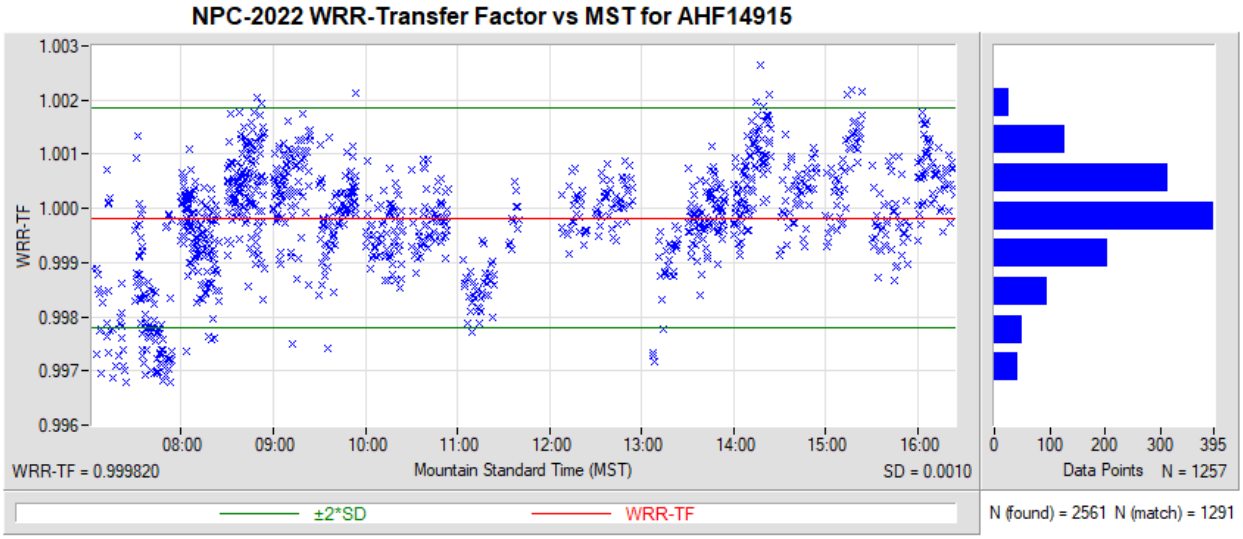

Figure 2. WRR-Transfer Factor vs. Mountain Standard Time for AHF14915

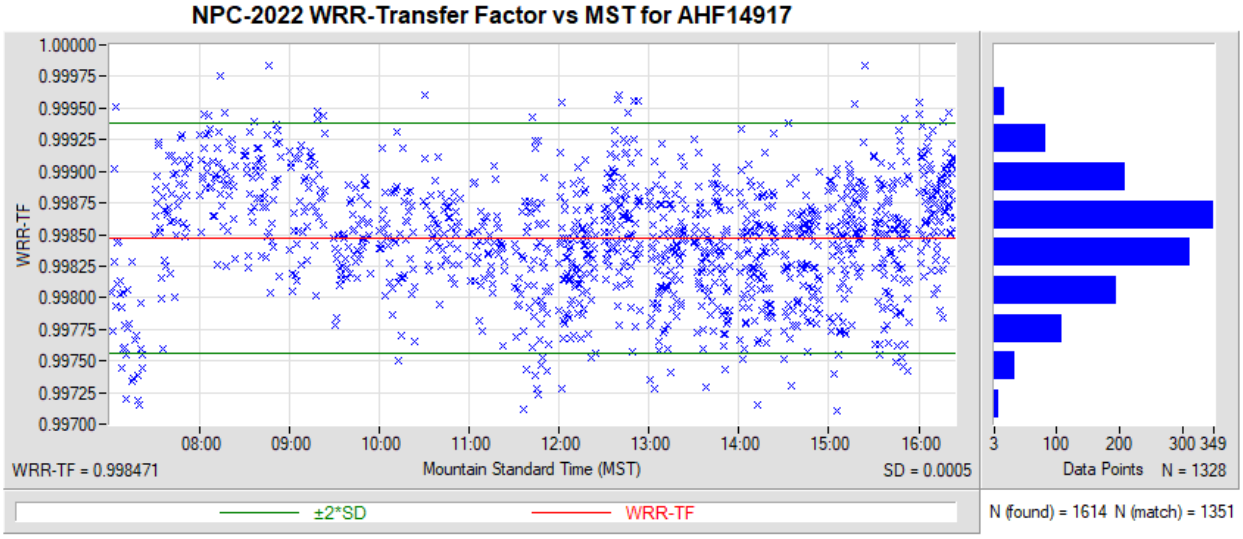

Figure 3. WRR-Transfer Factor vs. Mountain Standard Time for AHF14917

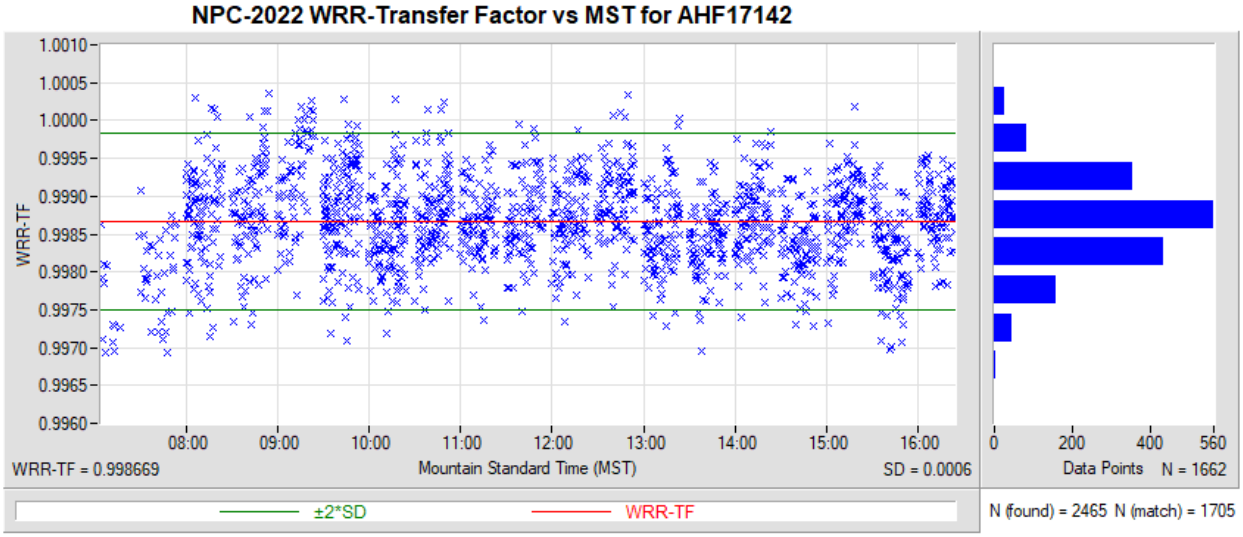

Figure 4. WRR-Transfer Factor vs. Mountain Standard Time for AHF17142

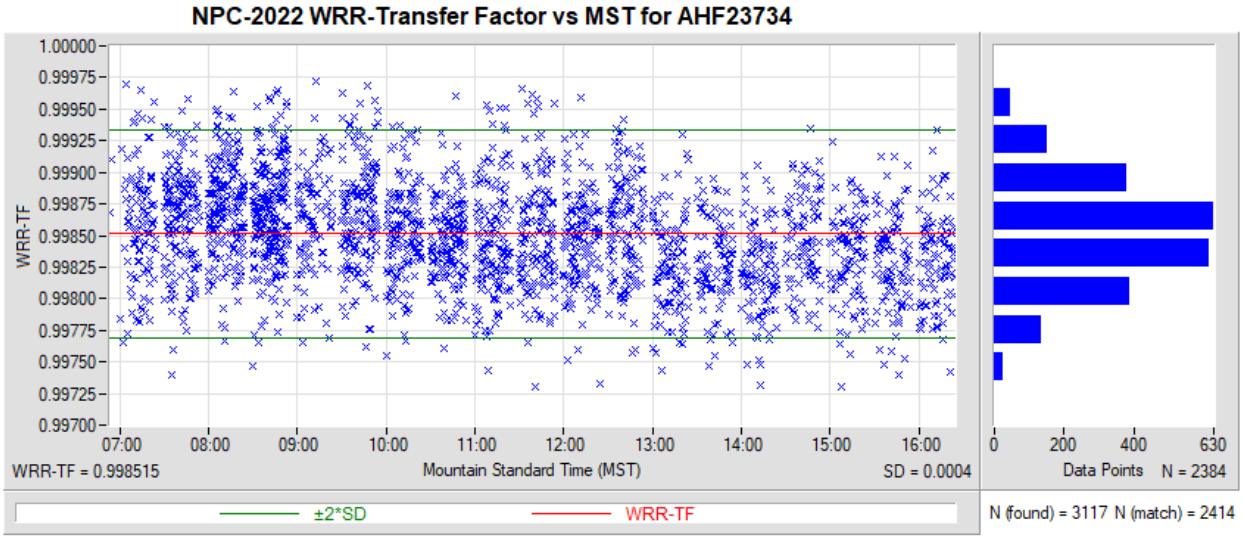

Figure 5. WRR-Transfer Factor vs. Mountain Standard Time for AHF23734

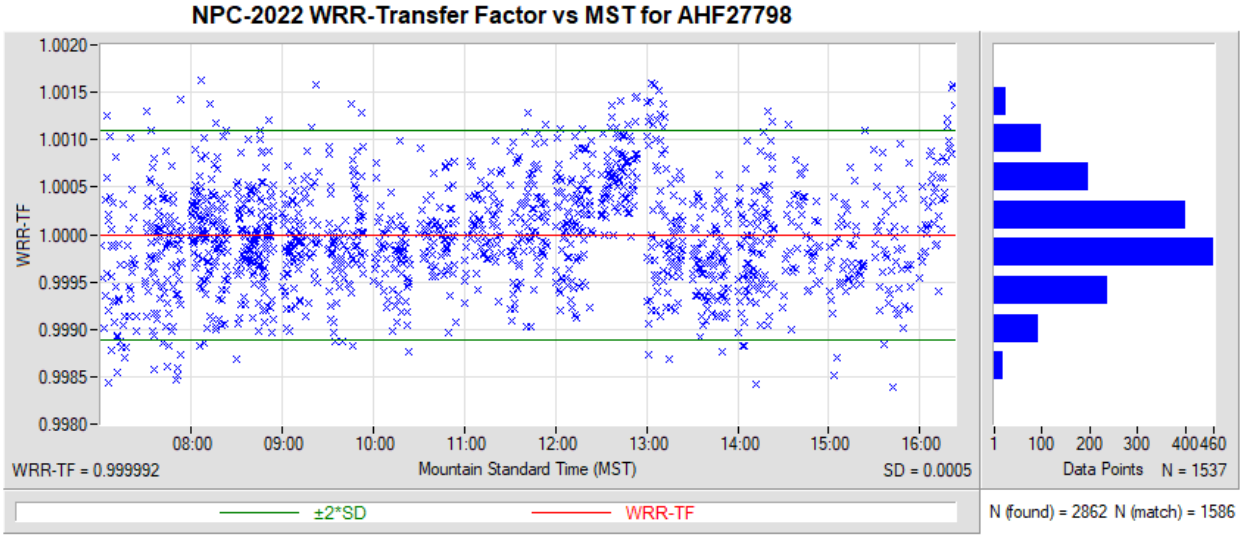

Figure 6. WRR-Transfer Factor vs. Mountain Standard Time for AHF27798

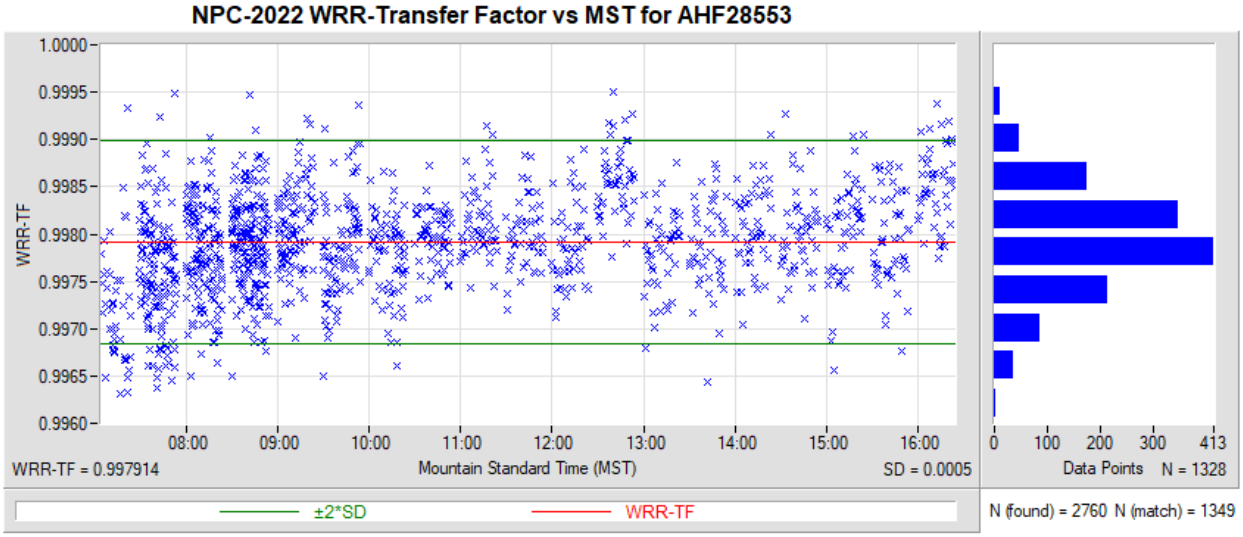

Figure 7. WRR-Transfer Factor vs. Mountain Standard Time for AHF28553

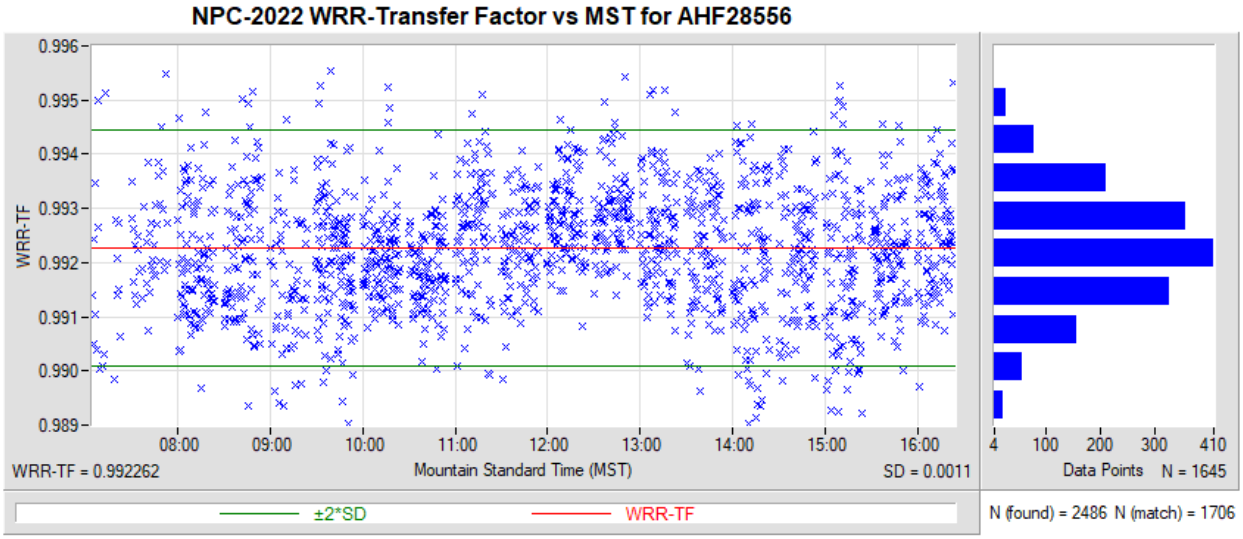

Figure 8. WRR-Transfer Factor vs. Mountain Standard Time for AHF28556

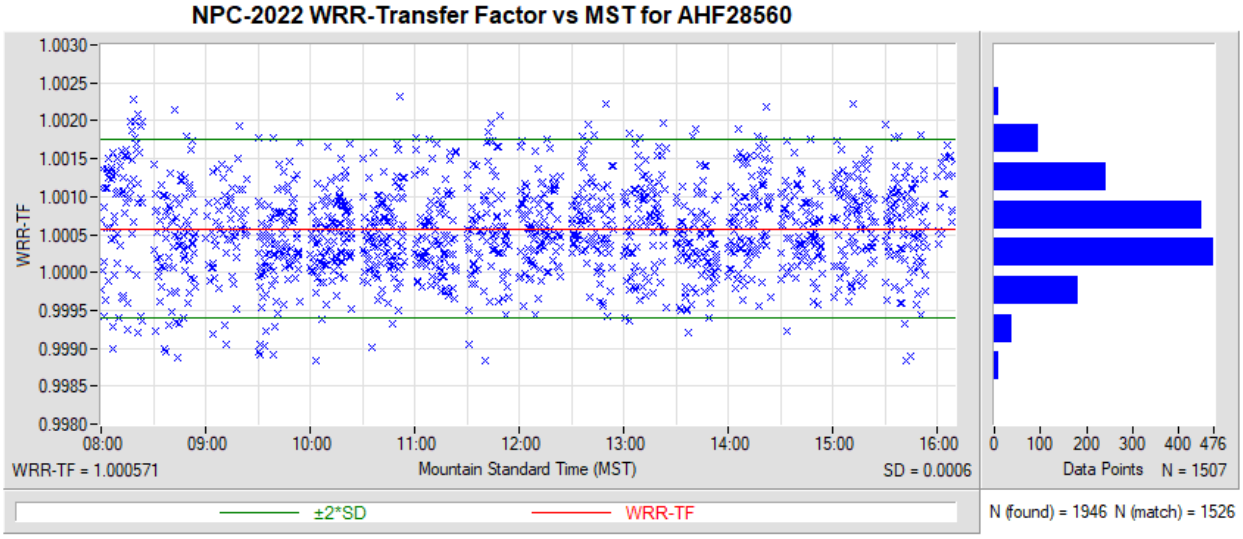

Figure 9. WRR-Transfer Factor vs. Mountain Standard Time for AHF28560

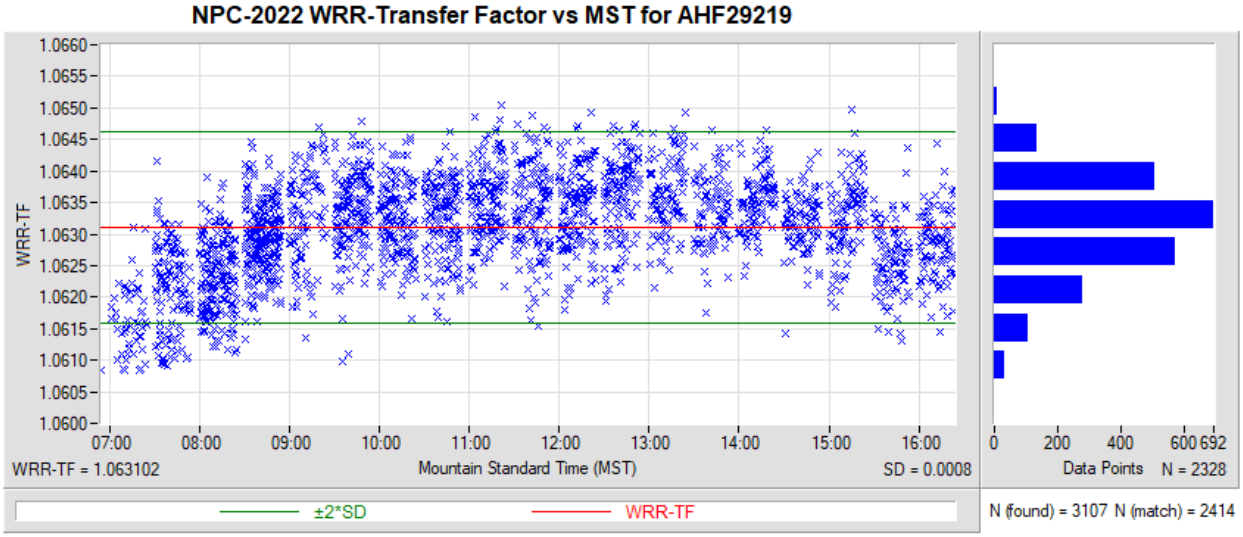

Figure 10. WRR-Transfer Factor vs. Mountain Standard Time for AHF29219

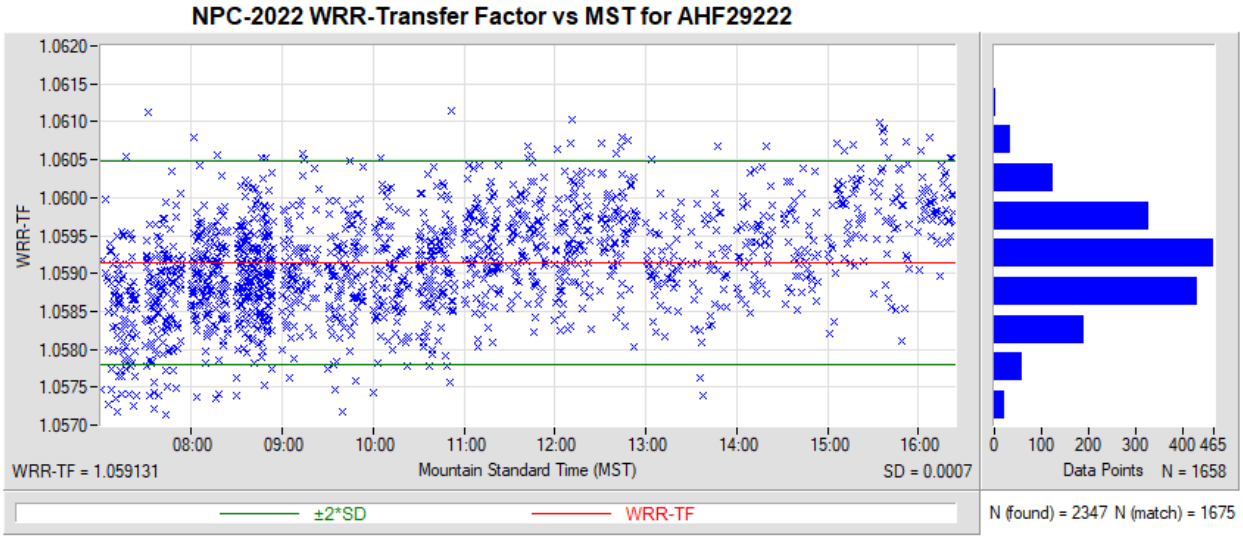

Figure 11. WRR-Transfer Factor vs. Mountain Standard Time for AHF29222

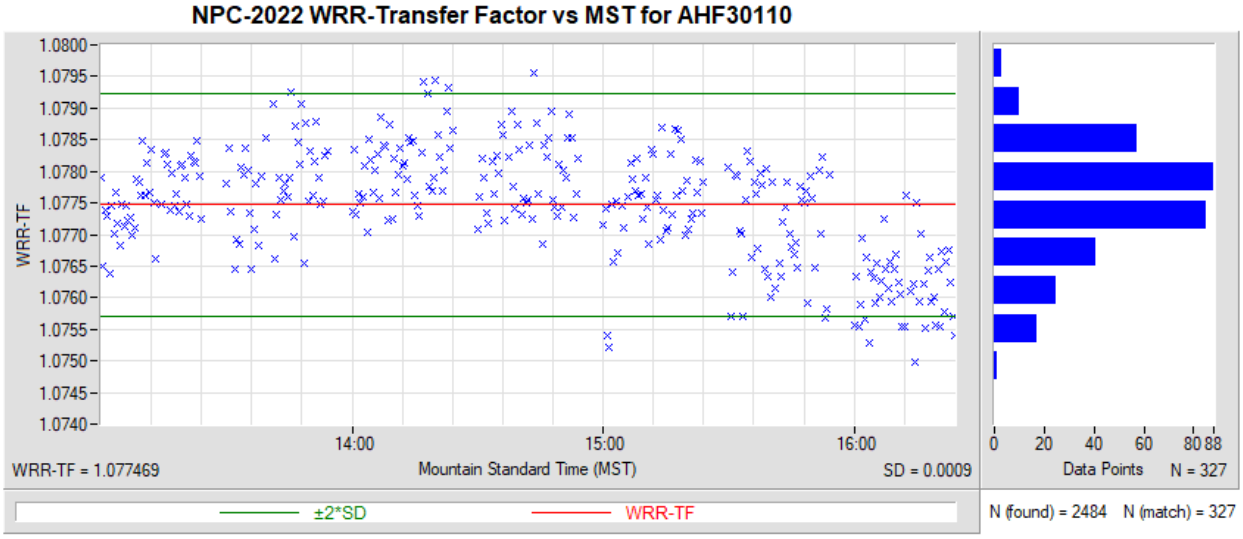

Figure 12. WRR-Transfer Factor vs. Mountain Standard Time for AHF30110

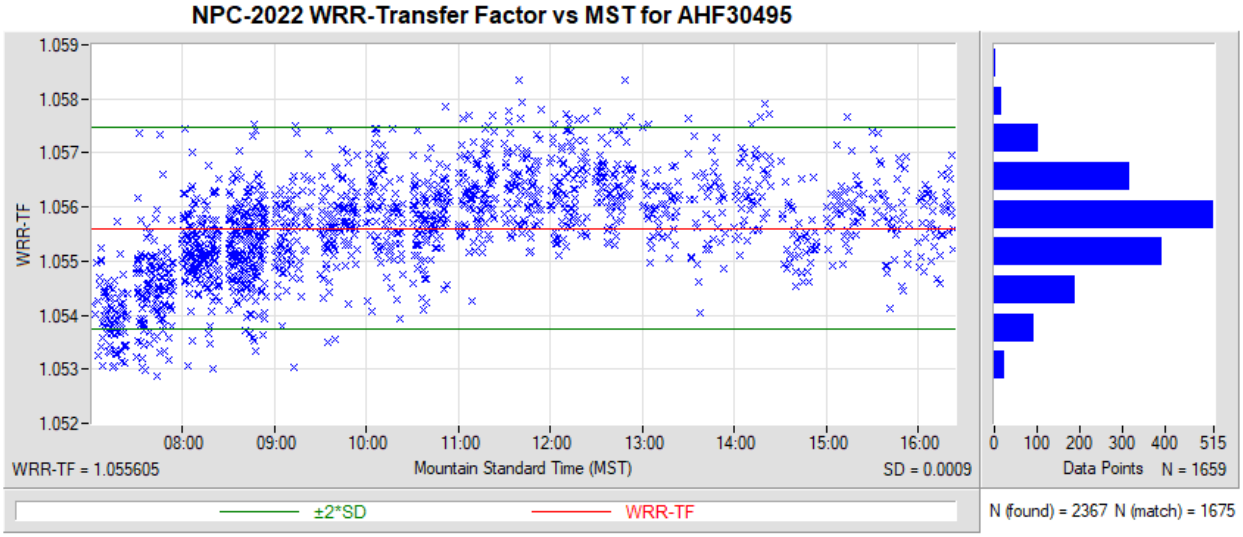

Figure 13. WRR-Transfer Factor vs. Mountain Standard Time for AHF30495

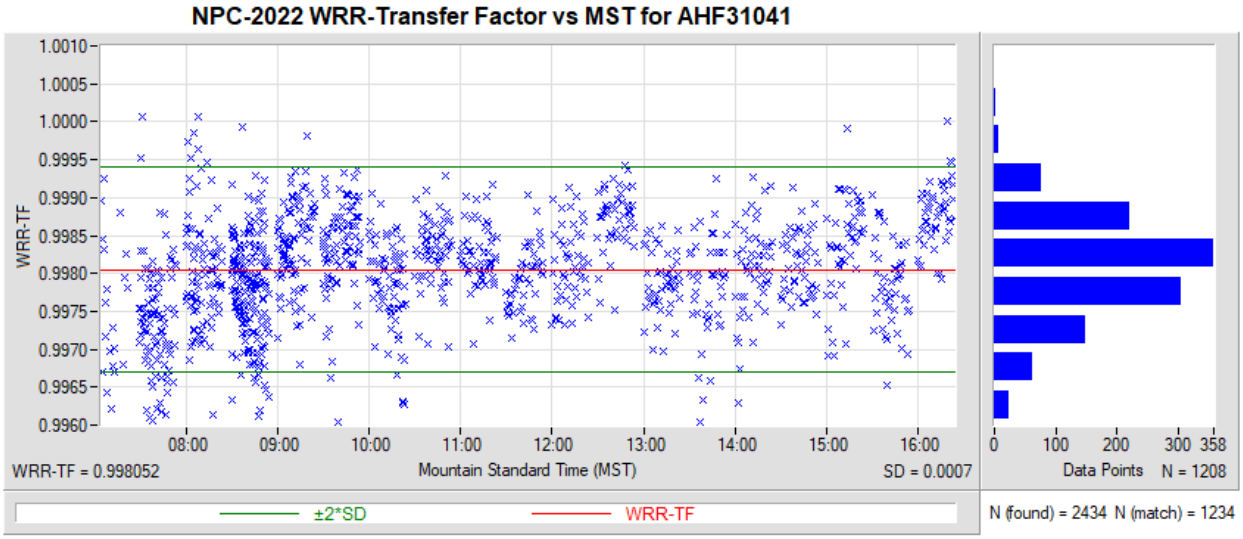

Figure 14. WRR-Transfer Factor vs. Mountain Standard Time for AHF31041

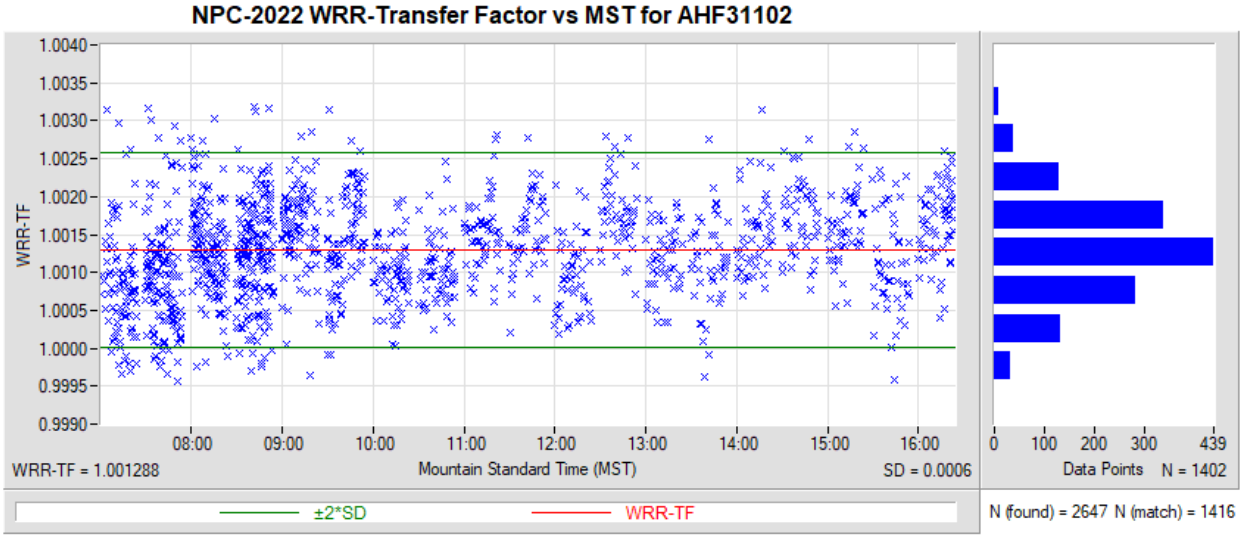

Figure 15. WRR-Transfer Factor vs. Mountain Standard Time for AHF31102

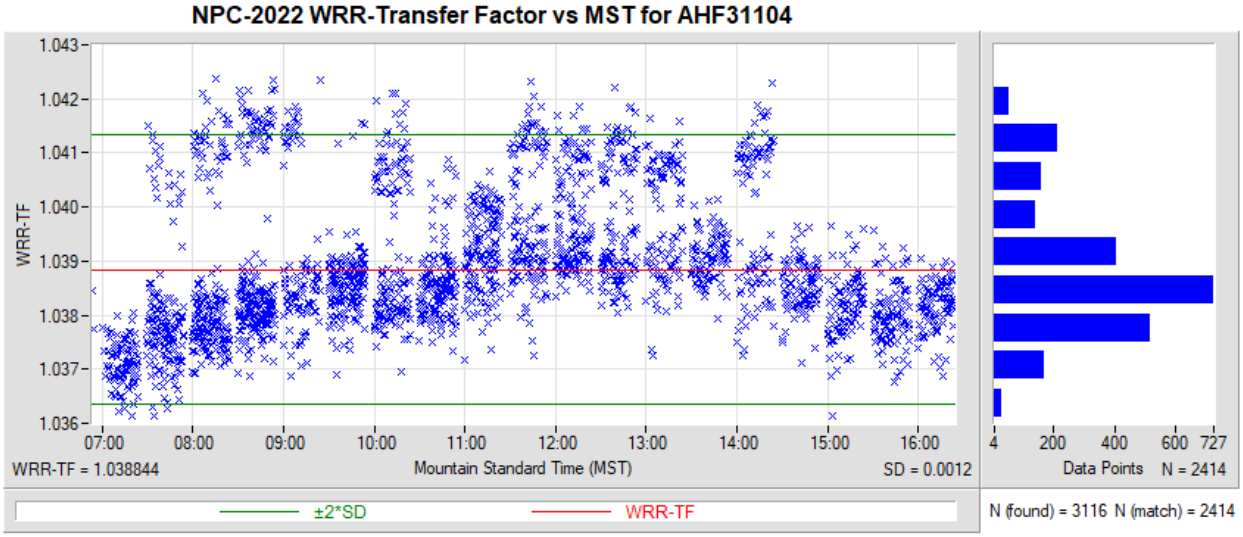

Figure 16. WRR-Transfer Factor vs. Mountain Standard Time for AHF31104

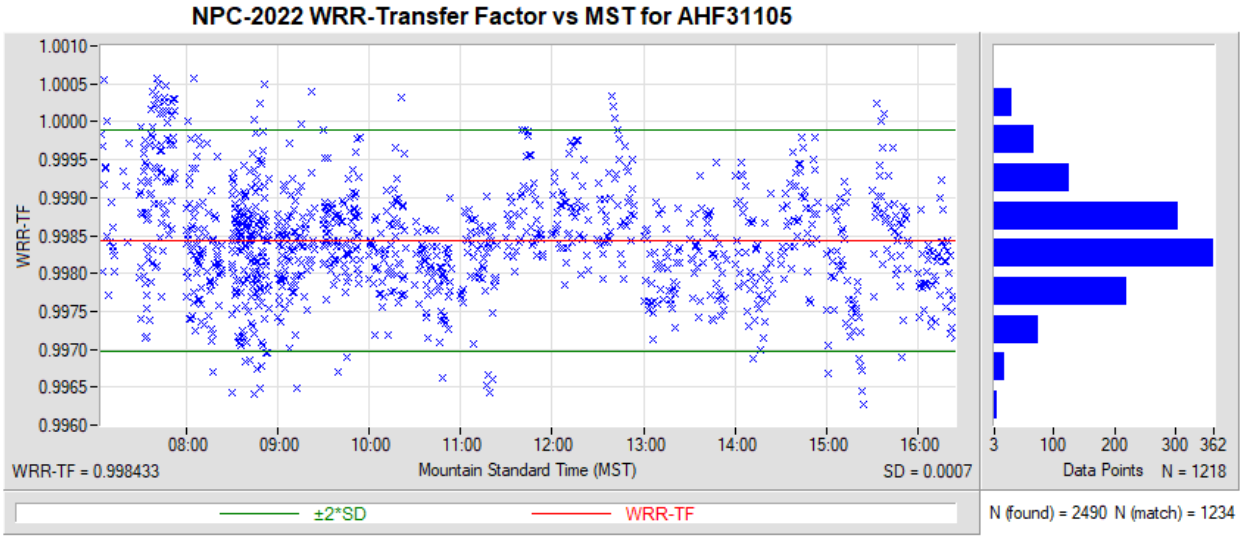

Figure 17. WRR-Transfer Factor vs. Mountain Standard Time for AHF31105

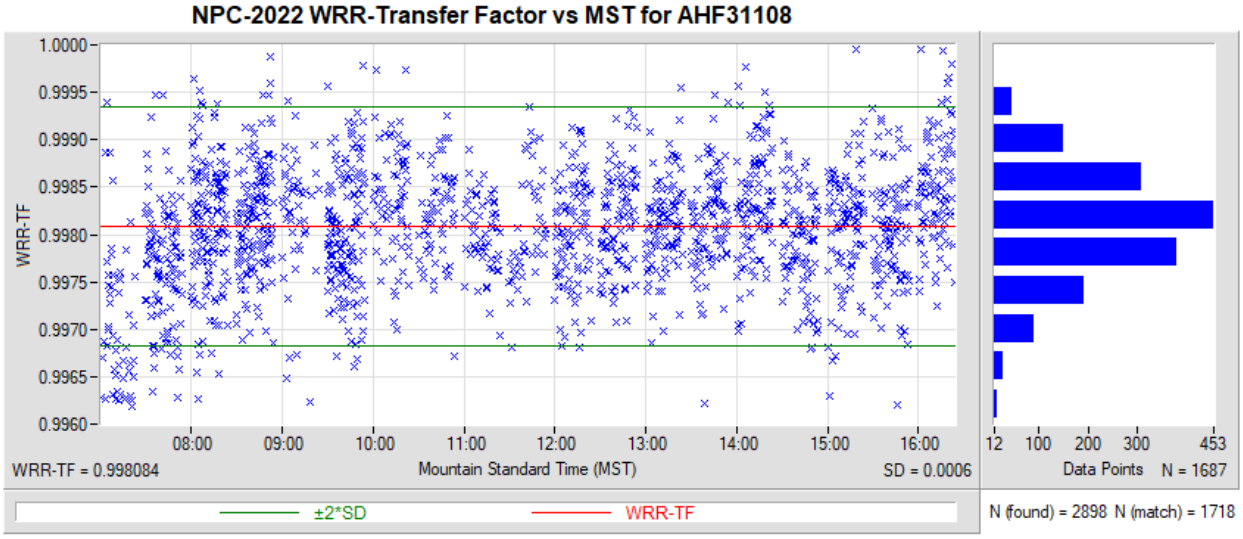

Figure 18. WRR-Transfer Factor vs. Mountain Standard Time for AHF31108

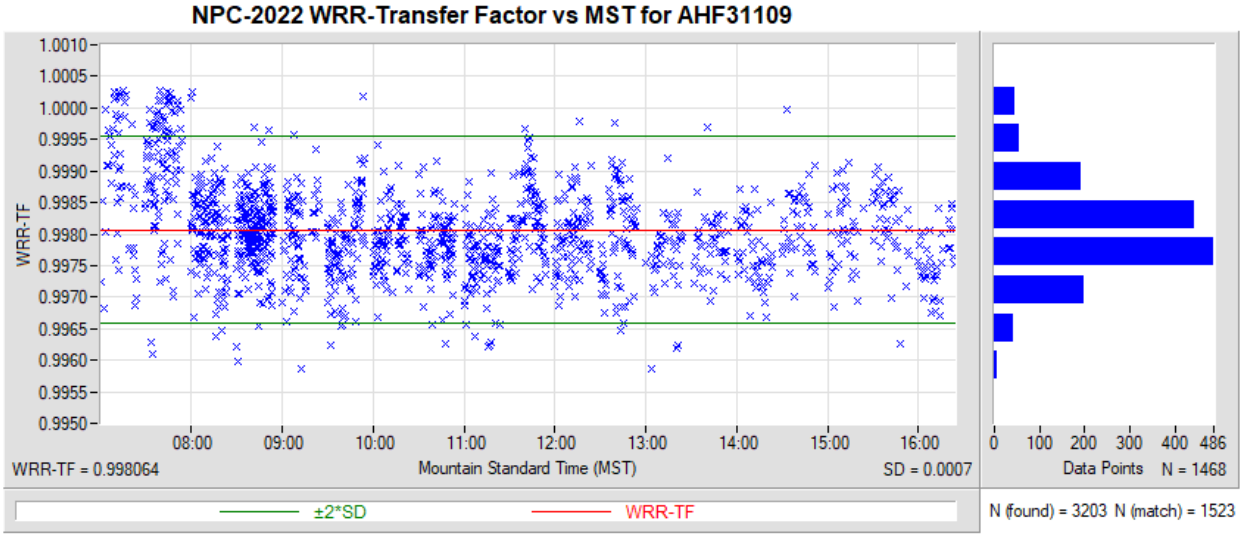

Figure 19. WRR-Transfer Factor vs. Mountain Standard Time for AHF31109

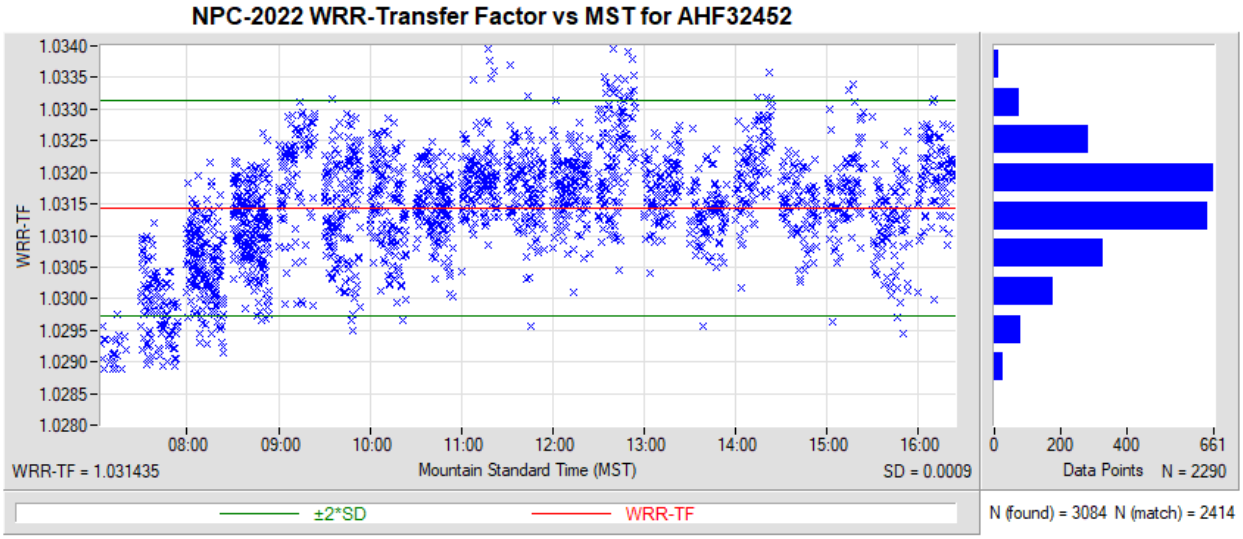

Figure 20. WRR-Transfer Factor vs. Mountain Standard Time for AHF32452

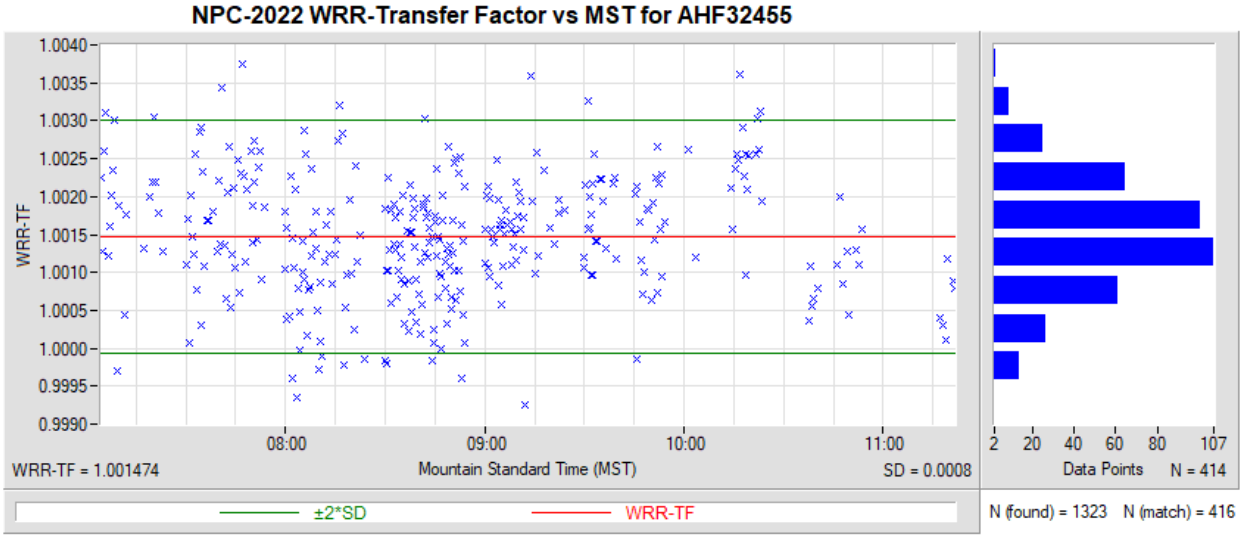

Figure 21. WRR-Transfer Factor vs. Mountain Standard Time for AHF32455

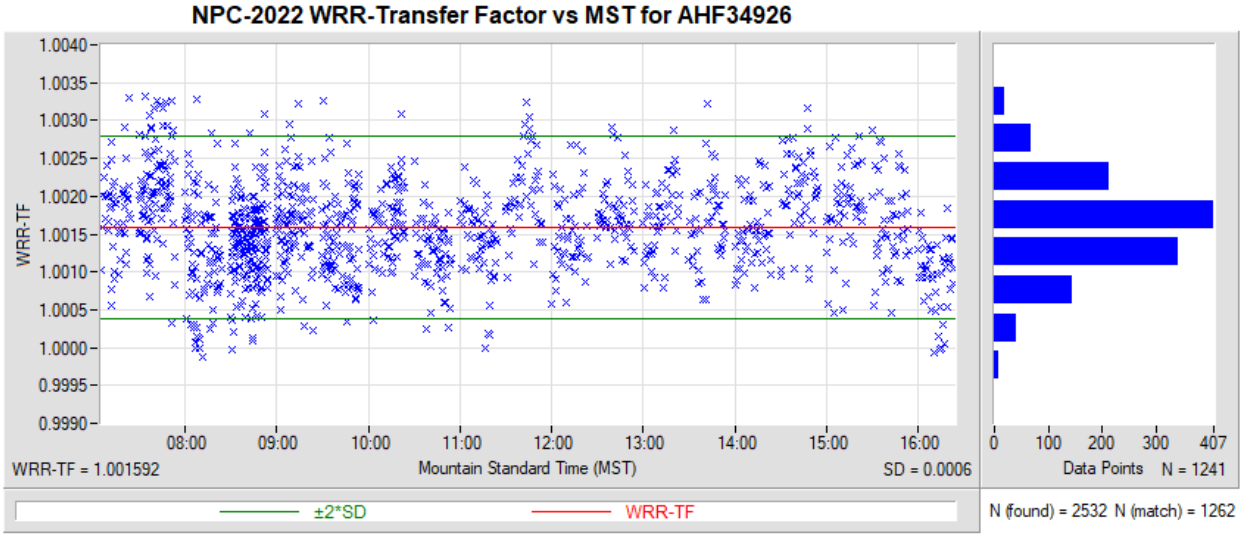

Figure 22. WRR-Transfer Factor vs. Mountain Standard Time for AHF34926

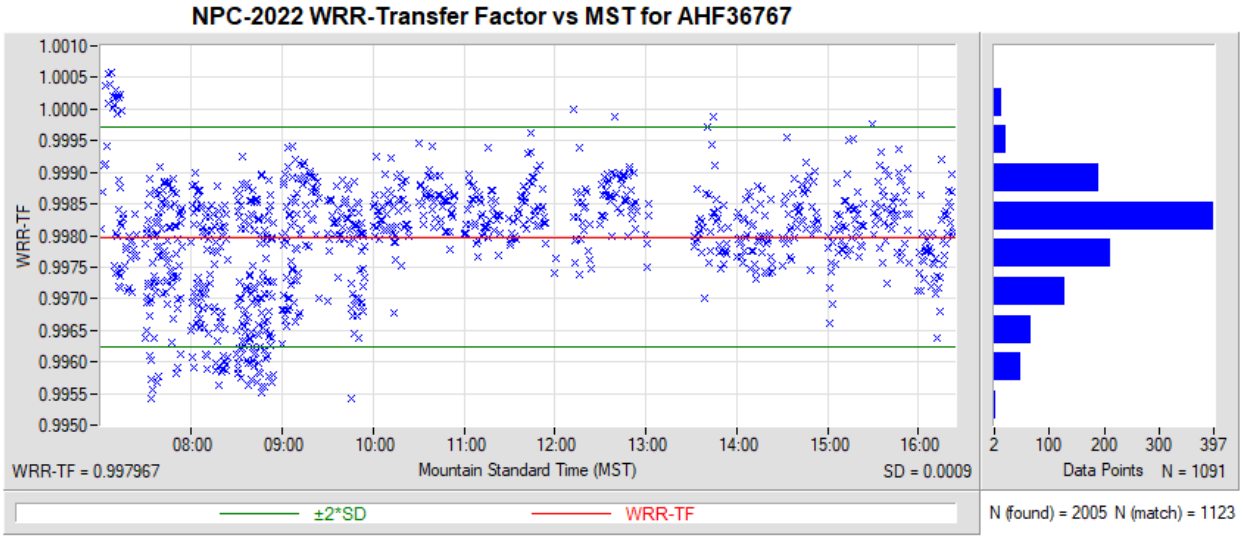

Figure 23. WRR-Transfer Factor vs. Mountain Standard Time for AHF36767

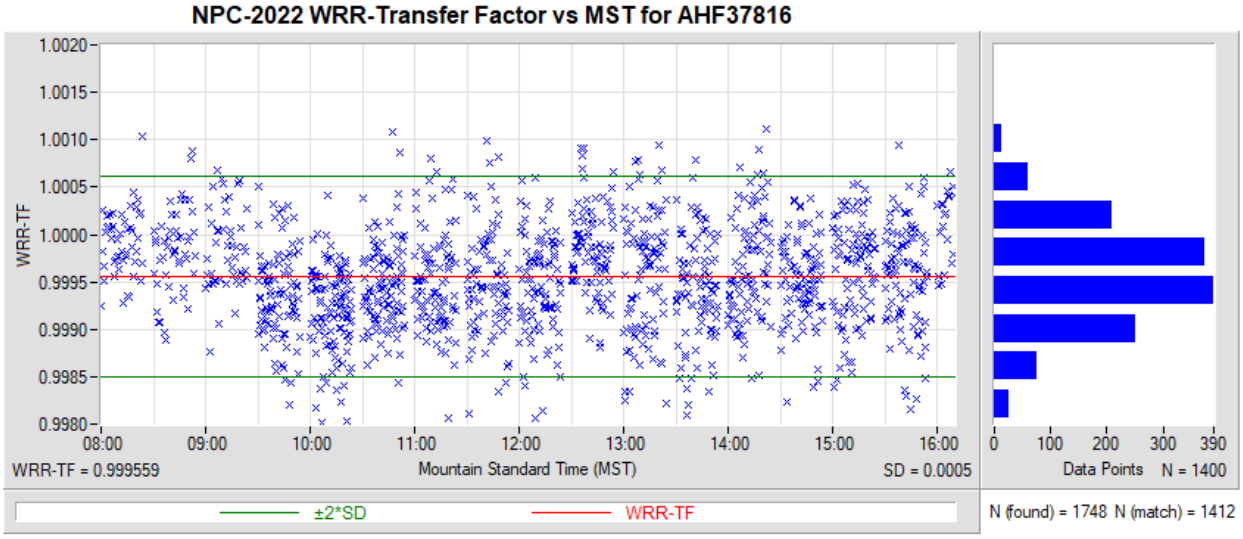

Figure 24. WRR-Transfer Factor vs. Mountain Standard Time for AHF37816

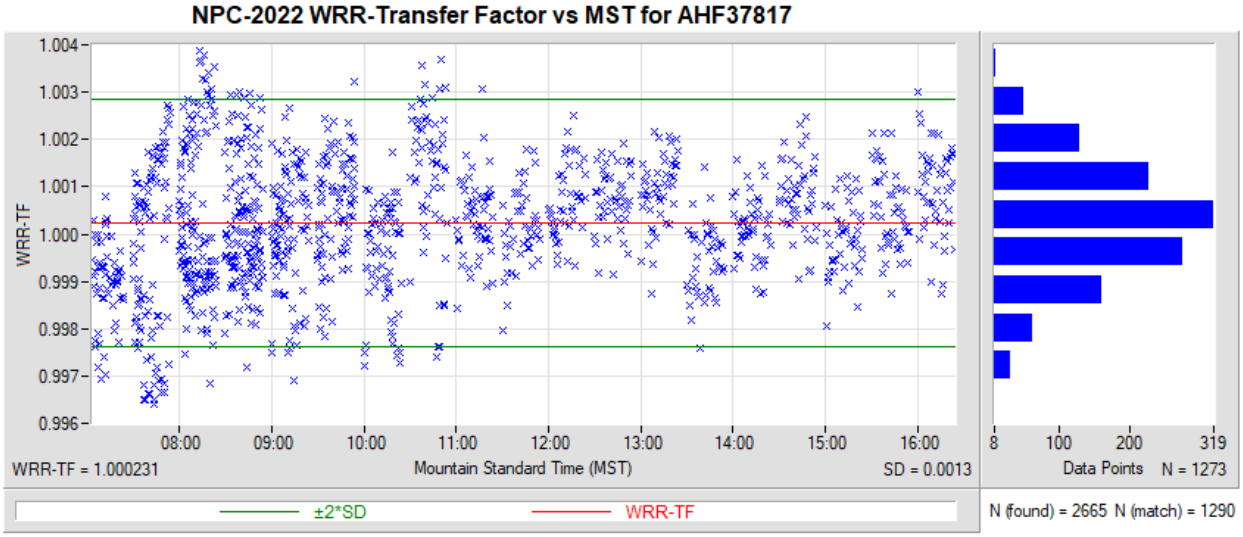

Figure 25. WRR-Transfer Factor vs. Mountain Standard Time for AHF37817

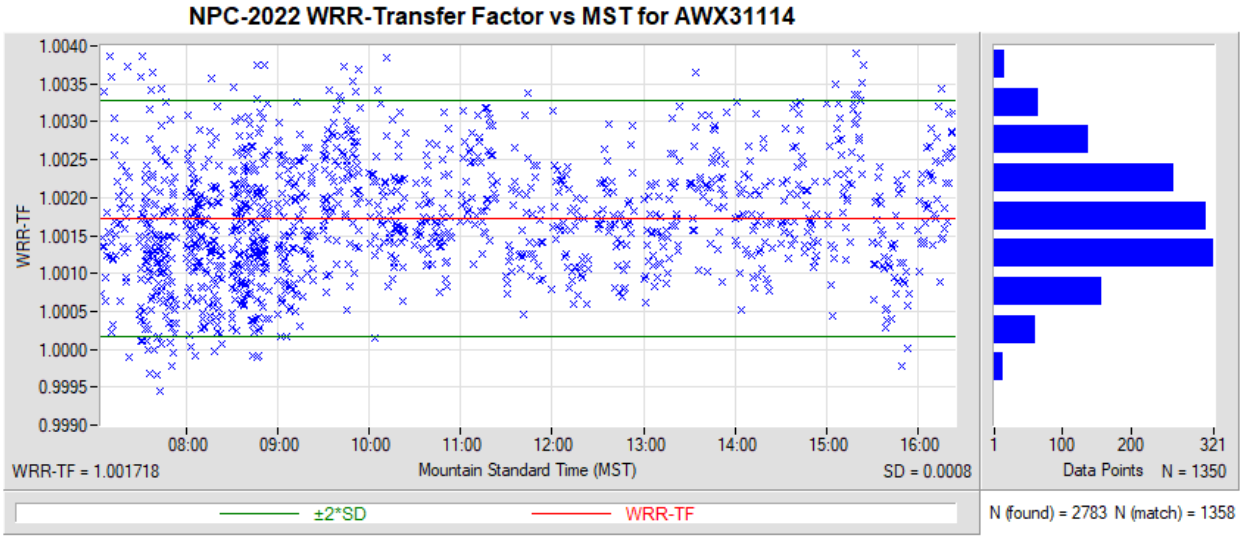

Figure 26. WRR-Transfer Factor vs. Mountain Standard Time for AWX31114

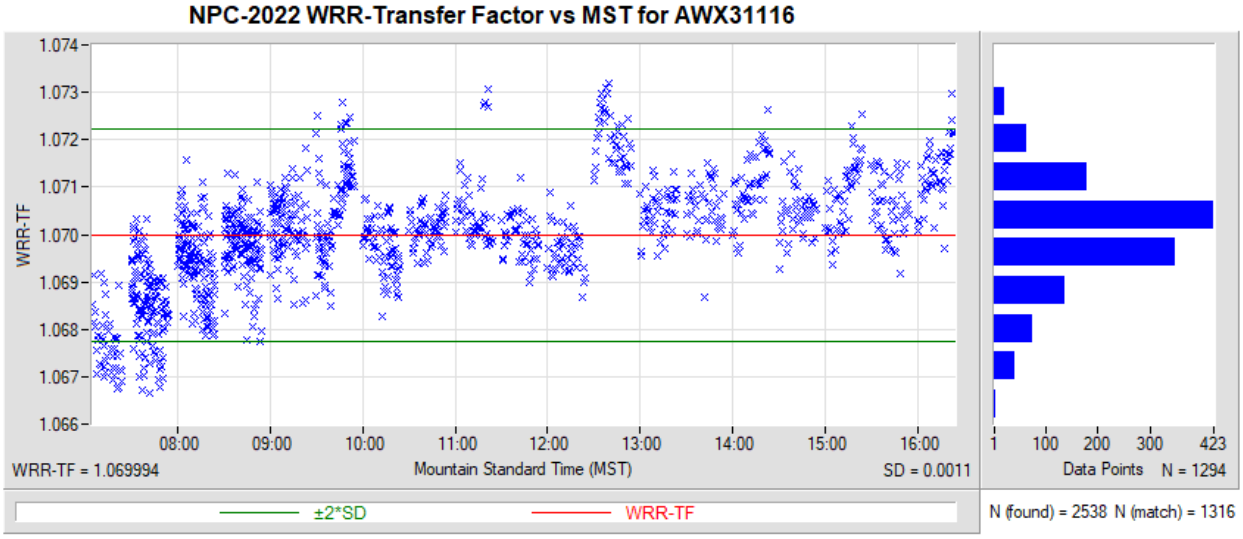

Figure 27. WRR-Transfer Factor vs. Mountain Standard Time for AWX31116

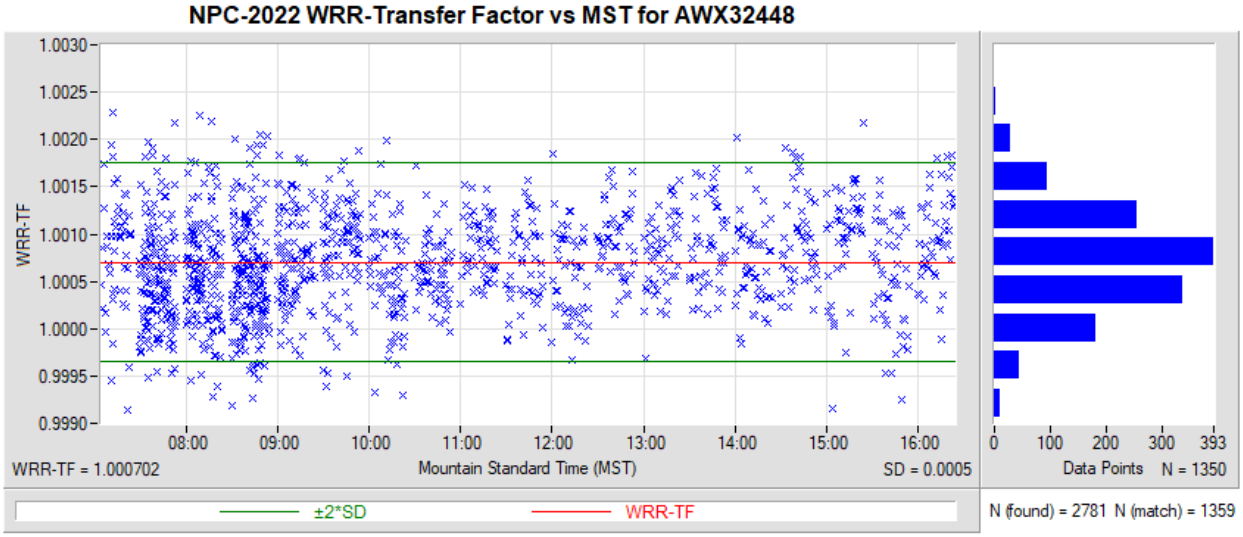

Figure 28. WRR-Transfer Factor vs. Mountain Standard Time for AWX32448

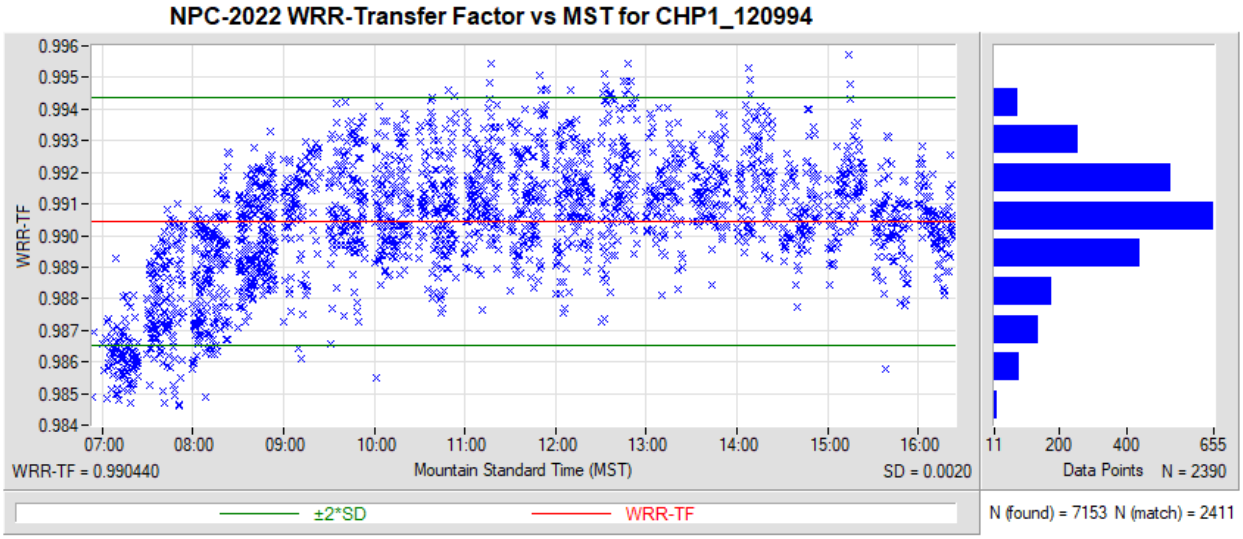

Figure 29. WRR-Transfer Factor vs. Mountain Standard Time for CHP1_120994

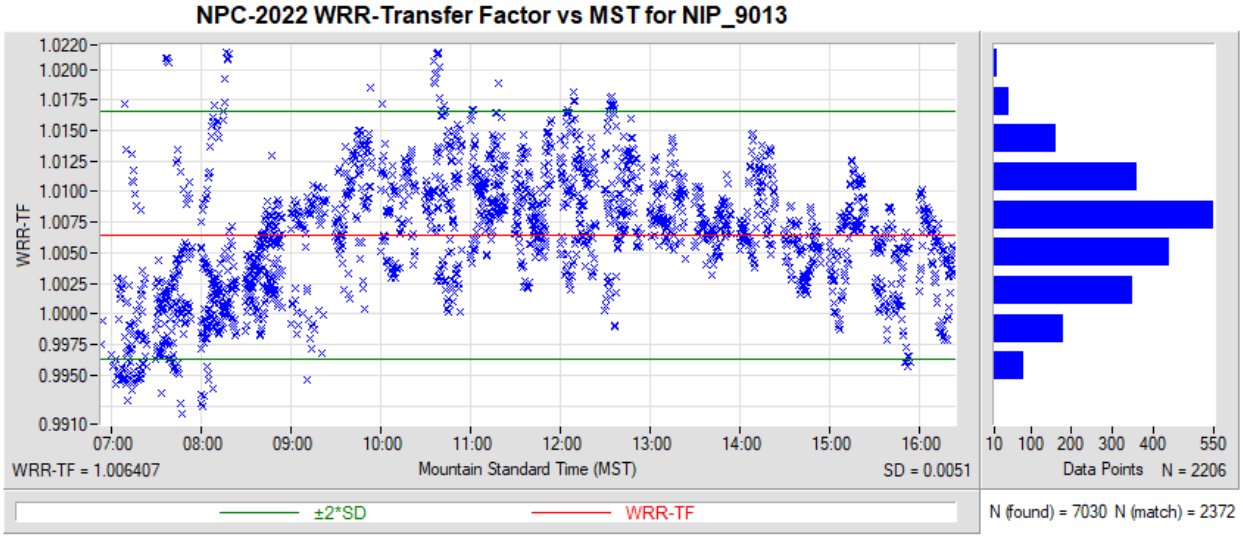

Figure 30. WRR-Transfer Factor vs. Mountain Standard Time for NIP_9013

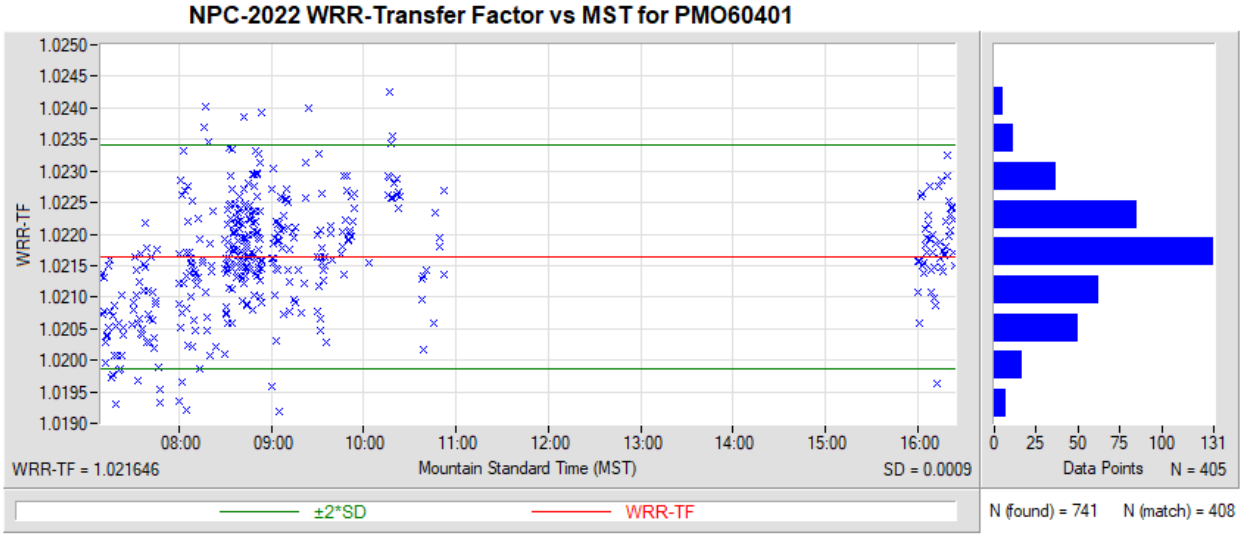

Figure 31. WRR-Transfer Factor vs. Mountain Standard Time for PMO6_0401

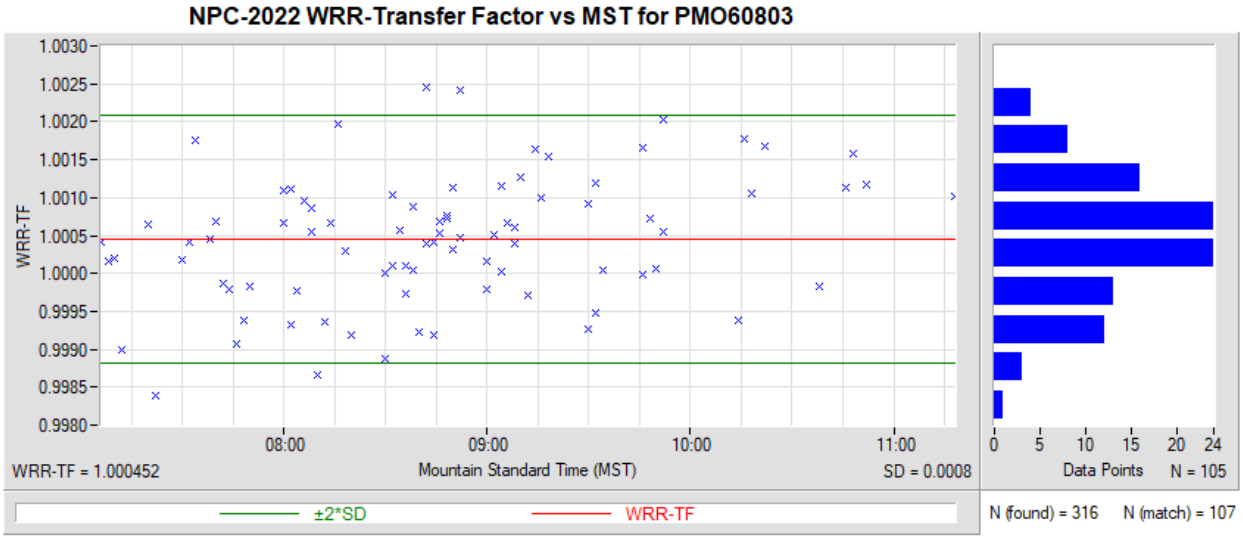

Figure 32. WRR-Transfer Factor vs. Mountain Standard Time for PMO6_0803

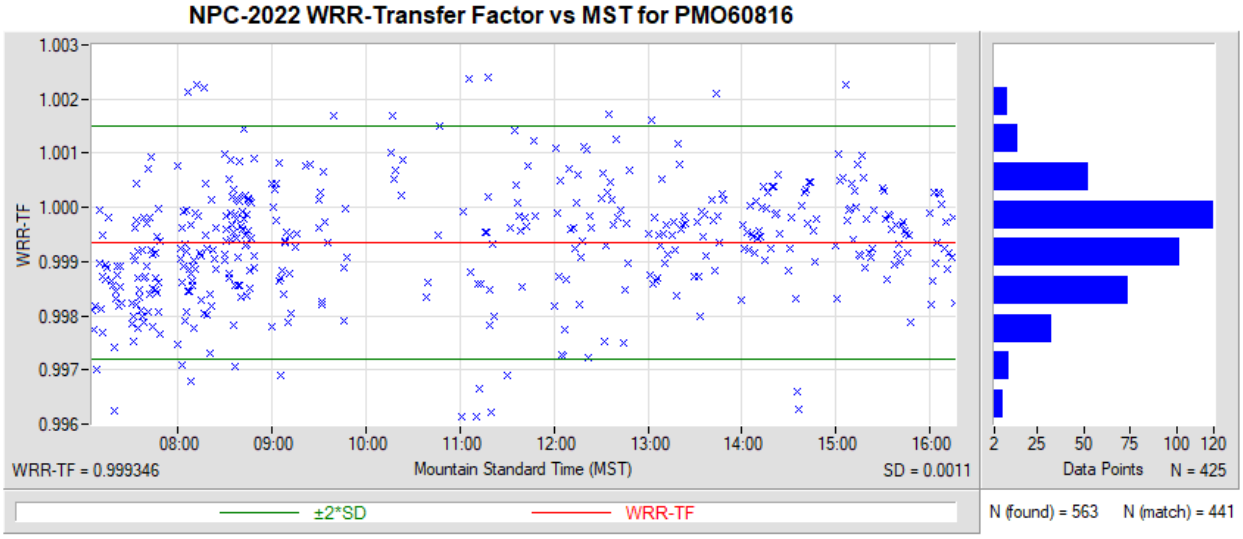

Figure 33. WRR-Transfer Factor vs. Mountain Standard Time for PMO6_0816

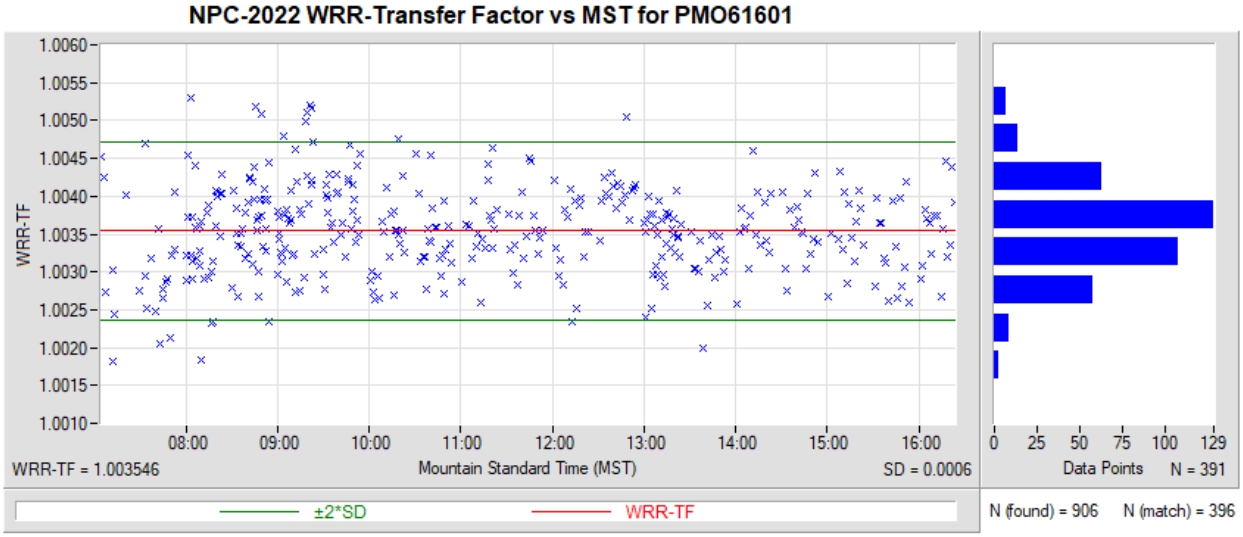

Figure 34. WRR-Transfer Factor vs. Mountain Standard Time for PMO6_1601

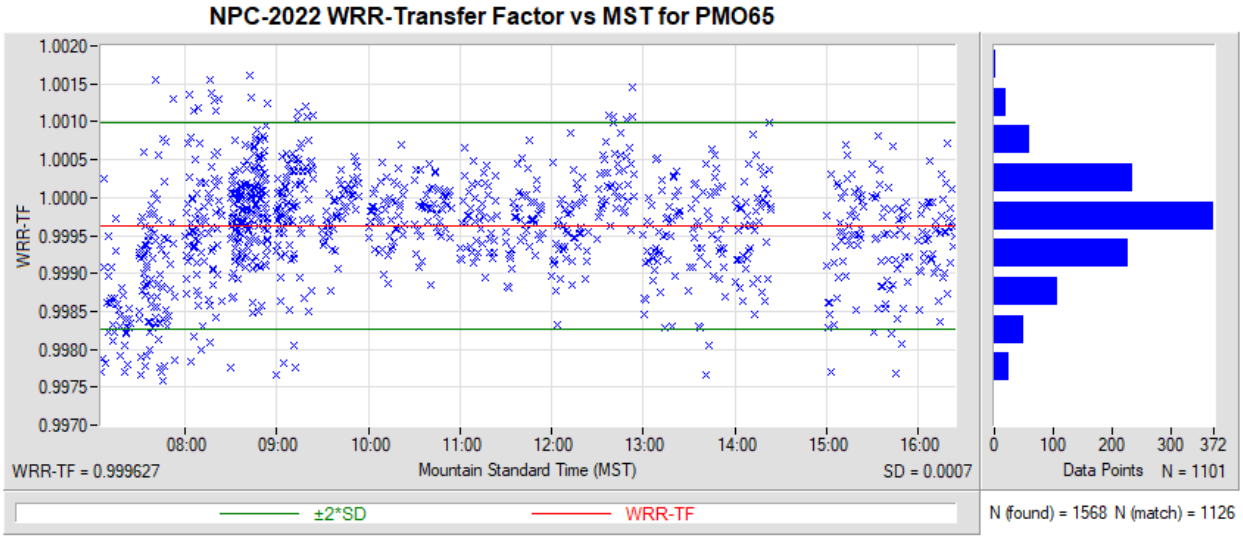

Figure 35. WRR-Transfer Factor vs. Mountain Standard Time for PMO6_5

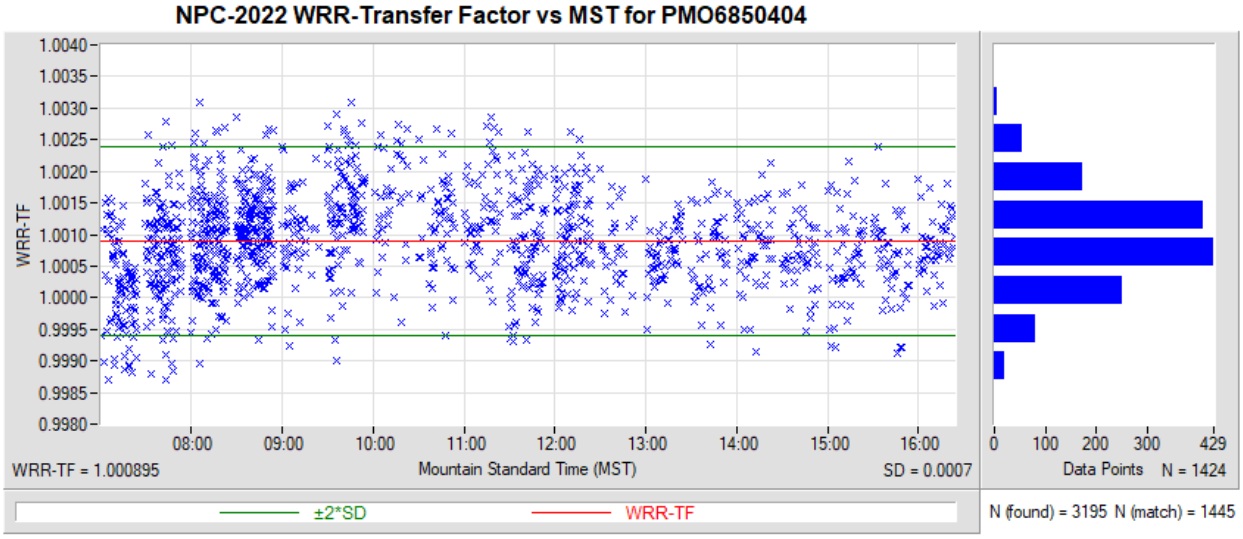

Figure 36. WRR-Transfer Factor vs. Mountain Standard Time for PMO6_850404

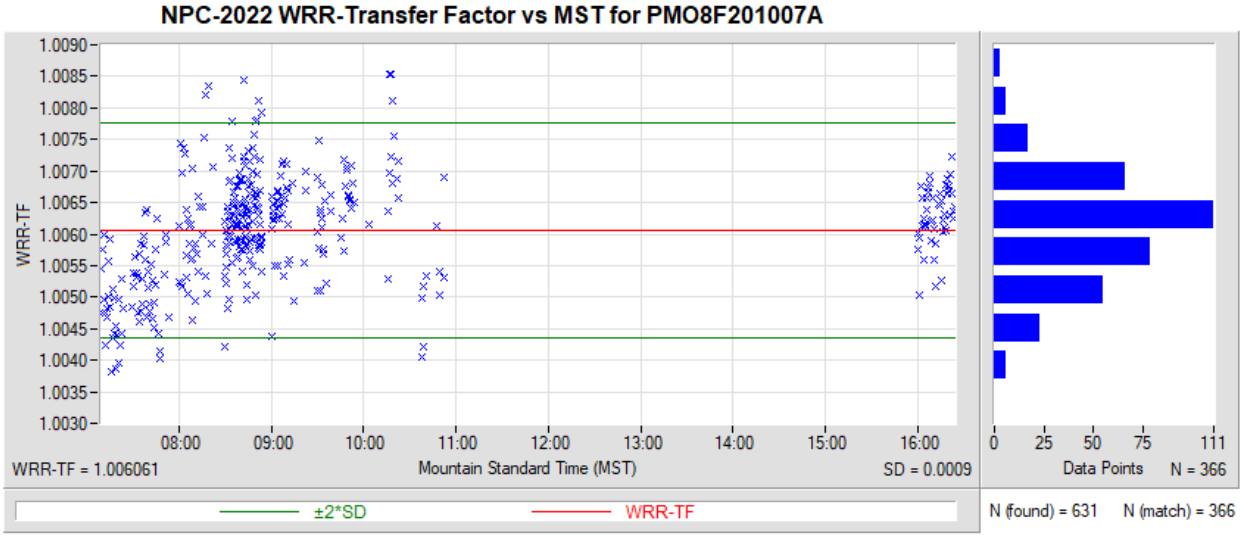

Figure 37. WRR-Transfer Factor vs. Mountain Standard Time for PMO8_F201007A

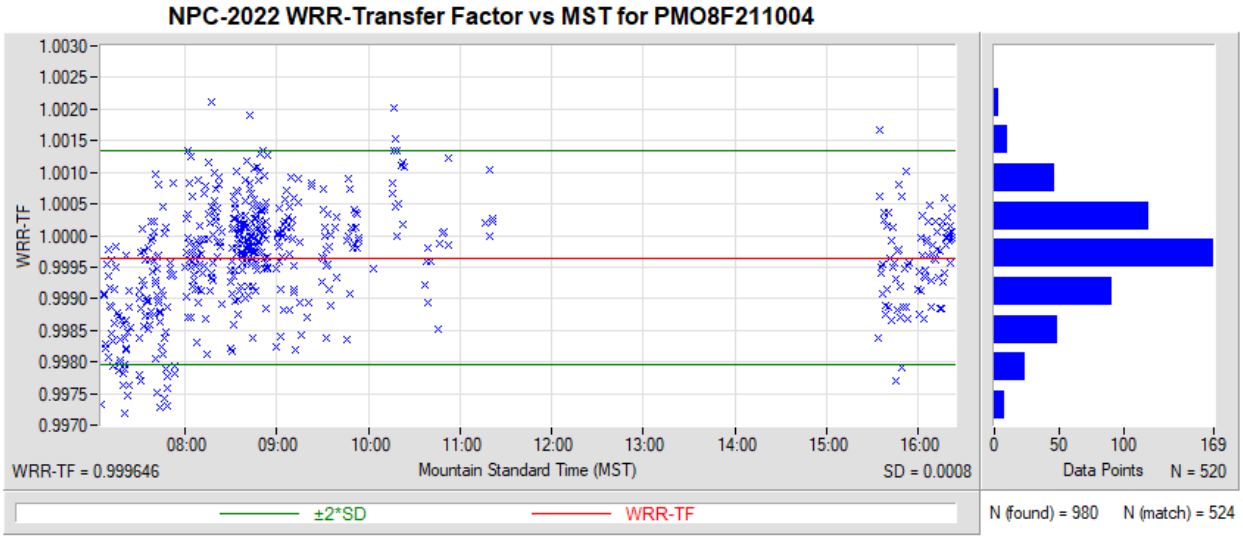

Figure 38. WRR-Transfer Factor vs. Mountain Standard Time for PMO8_F211004

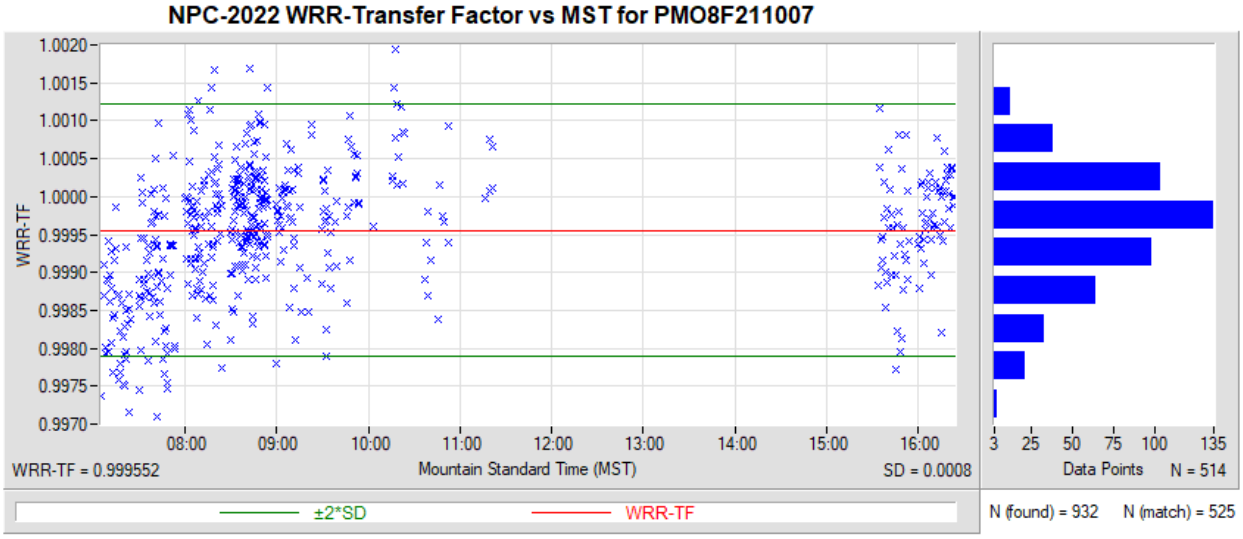

Figure 39. WRR-Transfer Factor vs. Mountain Standard Time for PMO8_F211007

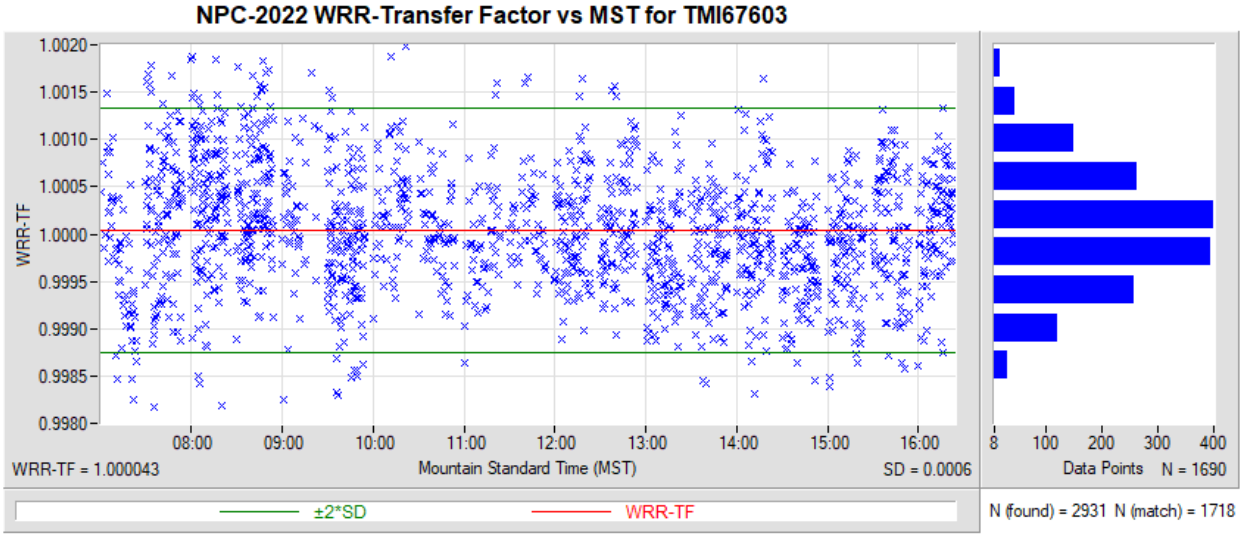

Figure 40. WRR-Transfer Factor vs. Mountain Standard Time for TMI67603

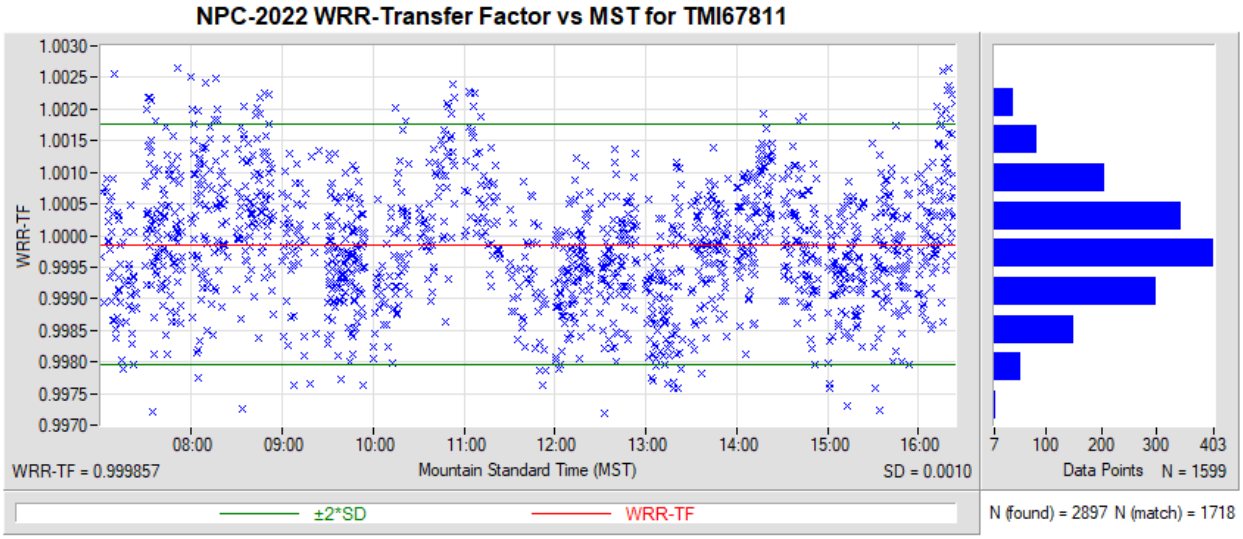

Figure 41. WRR-Transfer Factor vs. Mountain Standard Time for TMI67811

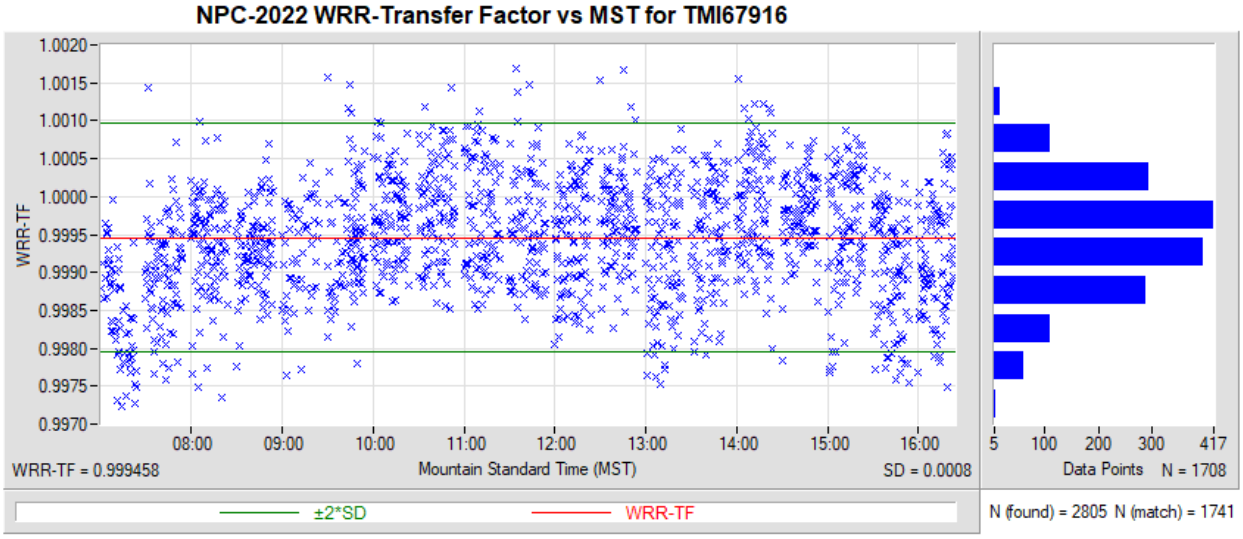

Figure 42. WRR-Transfer Factor vs. Mountain Standard Time for TMI67916

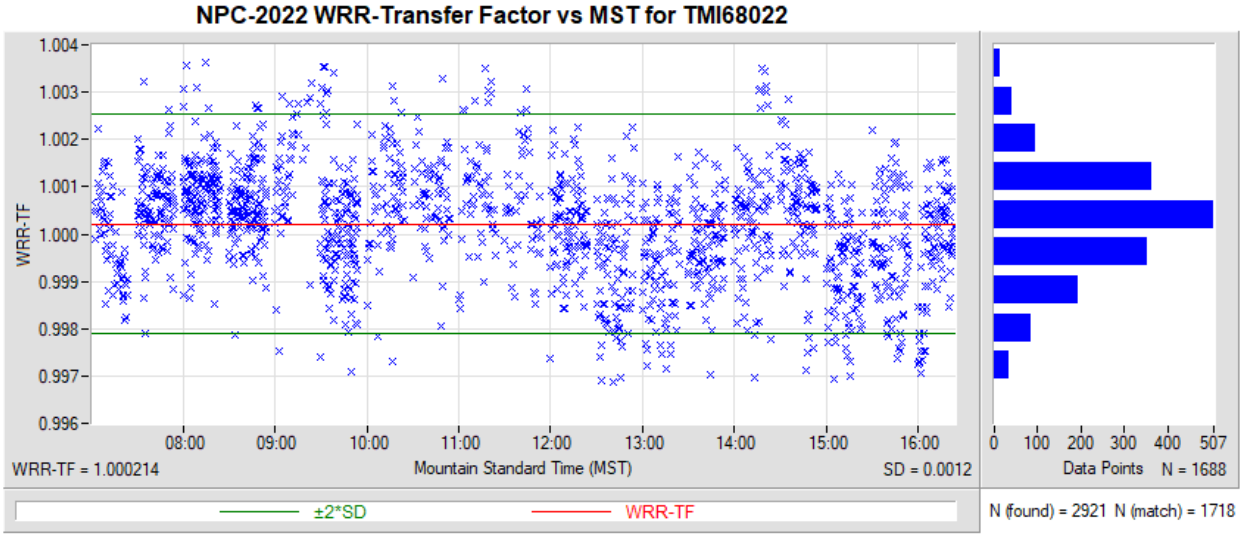

Figure 43. WRR-Transfer Factor vs. Mountain Standard Time for TMI68022

Table 4. Summary of Percent Change for Radiometers with a known WRR from a previous year

Cavity	WRR (NPC-2022)	WRR (previous)	Previous Year	%Change
AHF14915	0.99982	0.99983	2021	-0.00
AHF17142	0.99867	0.99828	2018	0.04
AHF23734	0.99851	0.99855	2021	-0.00
AHF27798	0.99999	1.00100	2021	-0.10
AHF28553	0.99791	0.99767	2019	0.02
AHF28556	0.99226	0.99056	2018	0.17
AHF28560	1.00057	1.00030	2021	0.03
AHF29219	1.06310	1.06142	2021	0.16
AHF29222	1.05913	1.05878	2021	0.03
AHF30110	1.07747	1.07222	2021	0.49
AHF30495	1.05561	1.05571	2021	-0.01
AHF31041	0.99805	0.99660	2019	0.15
AHF31102	1.00129	1.00052	2019	0.08
AHF31104	1.03884	1.03864	2021	0.02
AHF31105	0.99843	0.99805	2019	0.04
AHF31108	0.99808	0.99742	2019	0.07
AHF31109	0.99806	0.99780	?	0.03
AHF32452	1.03144	1.03125	2021	0.02
AHF32455	1.00147	1.00147	2021	0.00
AHF34926	1.00159	1.00136	2021	0.02
AHF37816	0.99956	0.99952	2021	0.00
AHF37817	1.00023	0.99902	?	0.12
AWX31114	1.00172	1.00141	2019	0.03
AWX31116	1.06999	1.06590	2019	0.38
AWX32448	1.00070	1.00030	2019	0.04
PMO6 0401	1.02165	1.02165	2021	-0.00
PMO6 0803	1.00045	1.00029	2021	0.02
PMO6 0816	0.99935	0.99919	2021	0.02
PMO6 1601	1.00355	1.00317	2019	0.04
PMO6 5	0.99963	0.99956	2021	0.01
PMO6 850404	1.00090	0.99803	?	0.29
PMO8 F201007A	1.00606	1.00633	2021	-0.03
TMI67603	1.00004	0.99987	2019	0.02
TMI67811	0.99986	0.99866	2018	0.12
TMI68022	1.00021	0.99996	2018	0.03

4.6 Recommendations

As a result of the comparisons made during NPC-2022, we suggest participants observe the following measurement practices:

- For the purpose of pyrheliometer comparisons, such as NPC-2022, we recommend the user apply only the manufacturer's calibration factor, not the WRR-TF or the new calibration factor, to report his or her absolute cavity radiometer's irradiance readings. Doing so eliminates the possibility of compounding WRR factors from previous comparisons.
- For data collection in the field, the manufacturer's calibration factor should be used to calculate the cavity responsivity. Each irradiance reading should then be *multiplied* by the appropriate WRR-TF to provide homogeneity of solar radiation measurements that are traceable to the WRR. We recommend this approach to realize the benefits of participating in the NPC.

5 Ancillary Data

The environmental conditions (i.e., temperature, relative humidity, barometric pressure, wind speed, precipitable water vapor, and spectral data) were measured during the NPC-2022 comparisons using the meteorological station at the SRRL. Additional information, including Baseline Measurement System data and graphical summaries, can be found on the Measurements and Instrumentation Data Center website.[5]

Time-series plots and other graphical presentations of these data collected during the pyrheliometer comparisons are presented in Appendix B.

[5] http:www.nrel.gov/midc/srrl_bms/

References

Finsterle, W. 2023. *WMO International Pyrheliometer Comparison, IPC-XIII, 27 September–15 October 2021: Final Report.* WMO IOM Report No. 140. Davos, Switzerland.

Fröhlich, C. 1991. "History of Solar Radiometry and the World Radiometric Reference." *Metrologia* 28(3): 111–115.

Reda, I. 1996. *Calibration of a Solar Absolute Cavity Radiometer With Traceability to the World Radiometric Reference.* Golden, CO: The National Renewable Energy Laboratory. NREL/TP-463-20619. https://doi.org/10.2172/15000940.

Reda, I., D. Myers, and T. Stoffel. 2008. "Uncertainty Estimate for the Outdoor Calibration of Solar Pyranometers: A Metrologist Perspective." *NCSLI Measure: The Journal of Measurement Science* 3(4): 58–66. https://doi.org/10.1080/19315775.2008.11721448.

Romero, J. 1995. *Direct Solar Irradiance Measurements with Pyrheliometers: Instruments and Calibrations. IPC-VIII.* Davos, Switzerland; 16 pp.

Romero, J., N.P. Fox, and C. Fröhlich. 1996. "Improved Comparison of the World Radiometric Reference and the SI Radiometric Scale." *Metrologia* 32(6): 523–524.

Physikalisch-Meteorologisches Observatorium Davos—World Radiation Center (PMOD/WRC). 1996. *International Pyrheliometer Comparison, IPC VIII, 25 September–13 October 1995, Results and Symposium.* Working Report No. 188. Davos Dorf, Switzerland: Swiss Meteorological Institute; 115 pp.

Appendix A. List of Participants and Pyrheliometers

Table A-1. List of Participants and Pyrheliometers

Operators	Affiliation	Radiometer Serial Number
Major McGee	Atlas Material Testing Technology	AHF17142, AHF28556
Matthew Perry	Campbell Scientific Inc.	PMO6-1601
Markus Suter	Davos Instruments AG	PMO6-0401, PMO8-F201-007A, PMO8-F211-004, PMO8-F211-007
Craig Webb, James Martin	DOE Atmospheric Radiation Measurement (ARM) Program	AHF30495, AHF29222
Akihito Akiyama, Dilip Ghimire, Jose Mario Po	EKO Instruments	PMO6-0816
Tom Kirk, Jim Wendell	Eppley Laboratory	AHF14915, AHF27798
Stefan Wacker	German Weather Service (DWD)	PMO6-5
Michael Donkers, Jorgen Konings	Hukseflux Thermal Sensors B.V.	n/a
Erik Naranen, Robert Dolce	ISO-Cal North America	AHF37816, AHF28560
Kun-Wei Lin, Bing-Qian Wu	Keelung Weather Station, Central Weather Bureau, Taiwan; National Central University, Taiwan	AHF31102
Abdullah Al Adwani, Abdullah Kalantan, Abdulmajeed Albabtin, Mohamad Almoamar	King Abdullah City for Atomic and Renewable Energy – KACARE	AHF30110
Nikhil Pattath Gopi	NATIONAL INSTITUTE OF SOLAR ENERGY, GURGAON, INDIA	AHF37817
Sankara Rao Tamada	NATIONAL INSTITUTE OF WIND ENERGY, CHENNAI, INDIA	AHF36767
Afshin Andreas, Mark Kutchenreiter	National Renewable Energy Laboratory (References)	AHF28968, AHF29220, AHF30713, TMI68018
Afshin Andreas, Mark Kutchenreiter	National Renewable Energy Laboratory	AHF23734, AHF29219, AHF31104, AHF32452
Emiel Hall, Allen Jordan	NOAA	AHF28553, AWX31114, AWX31116, AWX32448
Don Nelson	NOAA	AHF14917
Wolfgang Finsterle	PMOD/WRC	PMO6-0803, AHF32455
Charles Robinson	Sandia National Laboratories	AHF31108, TMI67603, TMI67811, TMI68022
Bryan Fabbri, Frederick Denn	Science Systems and Applications Inc / NASA Langley	AHF31041, AHF31105
Julian Lell	Servicio Meteorológico Nacional	TMI67916
Brighton Mabasa	South African Weather Services	PMO6-850404, AHF31109
Akram Essnid	The Libyan Center for Solar Energy Research and Studies	NIP-9013
Agustin Laguarda Cirigliano	Universidad de la República, Laboratorio de Energía Solar	CHP1-120994
Josh Peterson	University of Oregon, Solar Radiation Monitoring Lab	AHF34926

Appendix B. Ancillary Data Summaries

The measurement performance of an ACR can be affected by several environmental parameters. Potentially relevant meteorological data collected during the NPC are presented in this appendix.

The Baseline Measurement System has been in continuous operation at the SRRL since 1981. Baseline Measurement System data are recorded as one-minute averages of three-second samples for each instrument.[6] Time-series plots and other graphical presentations of these data acquired during the NPC-2022 measurements are presented here.

[6] Additional information about the SRRL and the Baseline Measurement System can be found on the Measurement and Instrumentation Data Center at https://midcdmz.nrel.gov/srrl_bms/.

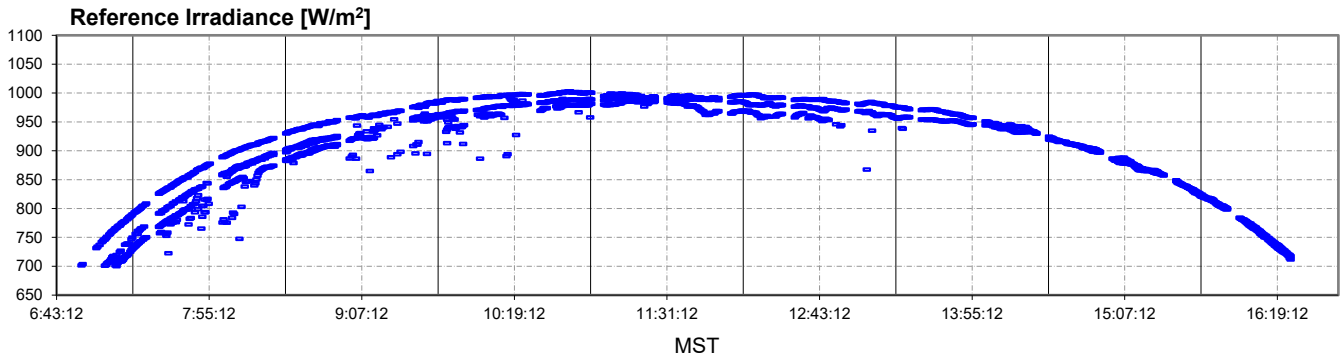

Figure B-1. Reference Irradiance (W/m^2) for 25 Sept – 1 Oct 2022

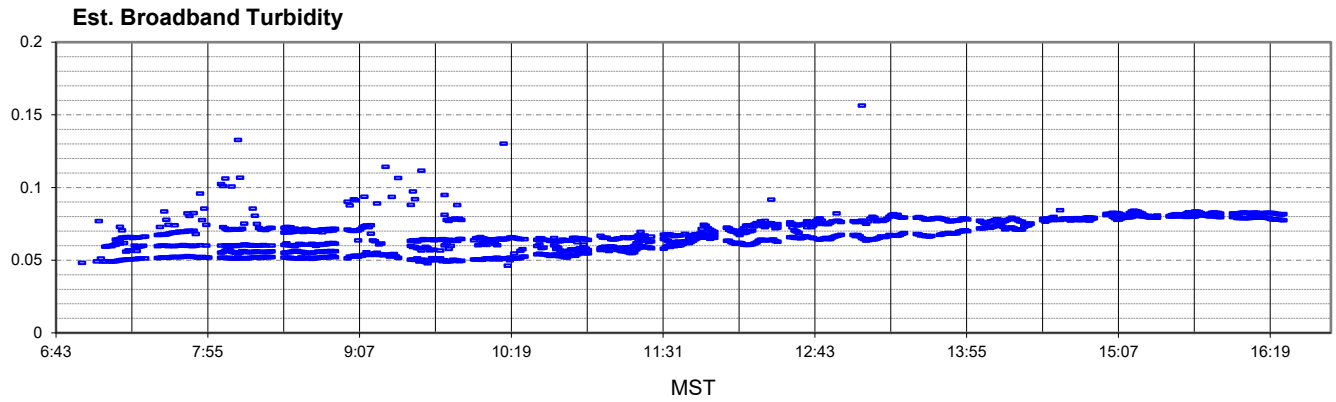

Figure B-2. Estimated broadband turbidity for 25 Sept – 1 Oct 2022

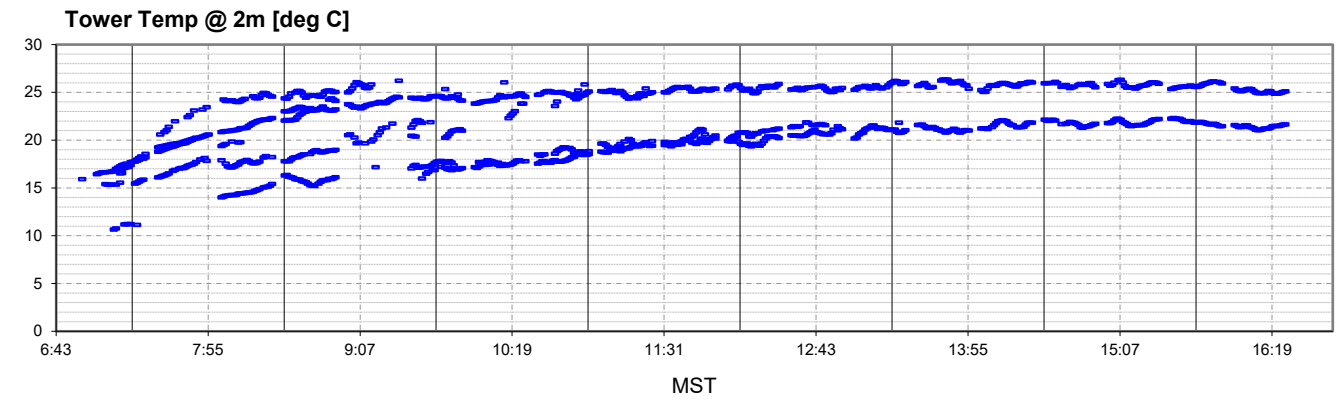

Figure B-3. Tower temperature at 2 m (ºC) for 25 Sept – 1 Oct 2022

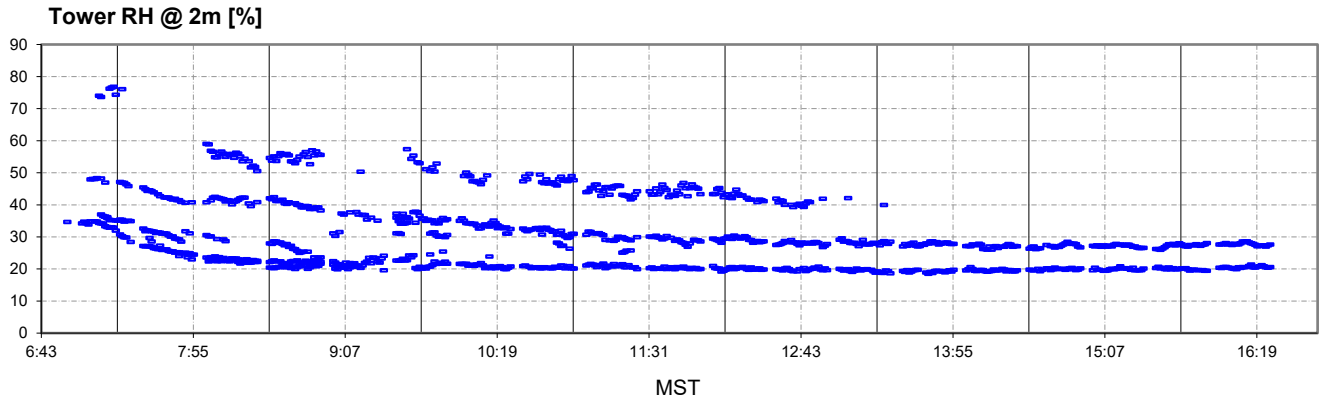

Figure B-4. Tower relative humidity at 2 m (%) for 25 Sept – 1 Oct 2022

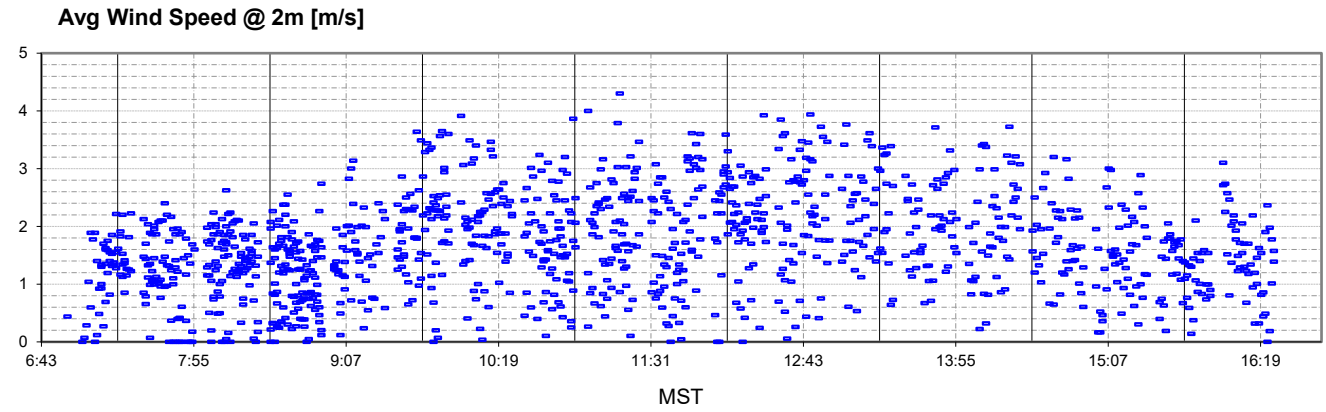

Figure B-5. Average wind speed at 2 m (m/s) for 25 Sept – 1 Oct 2022

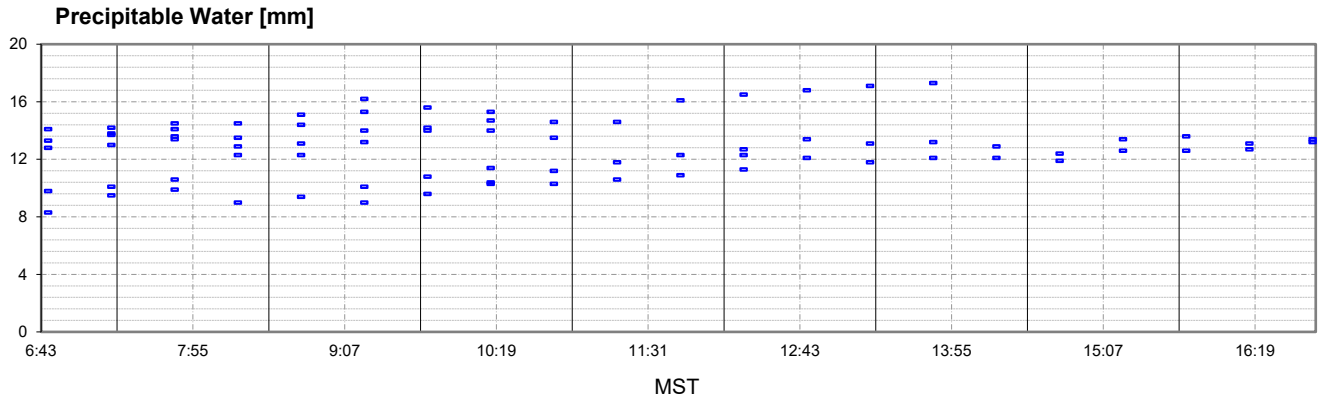

Figure B-6. Precipitable water (mm) for 25 Sept – 1 Oct 2022

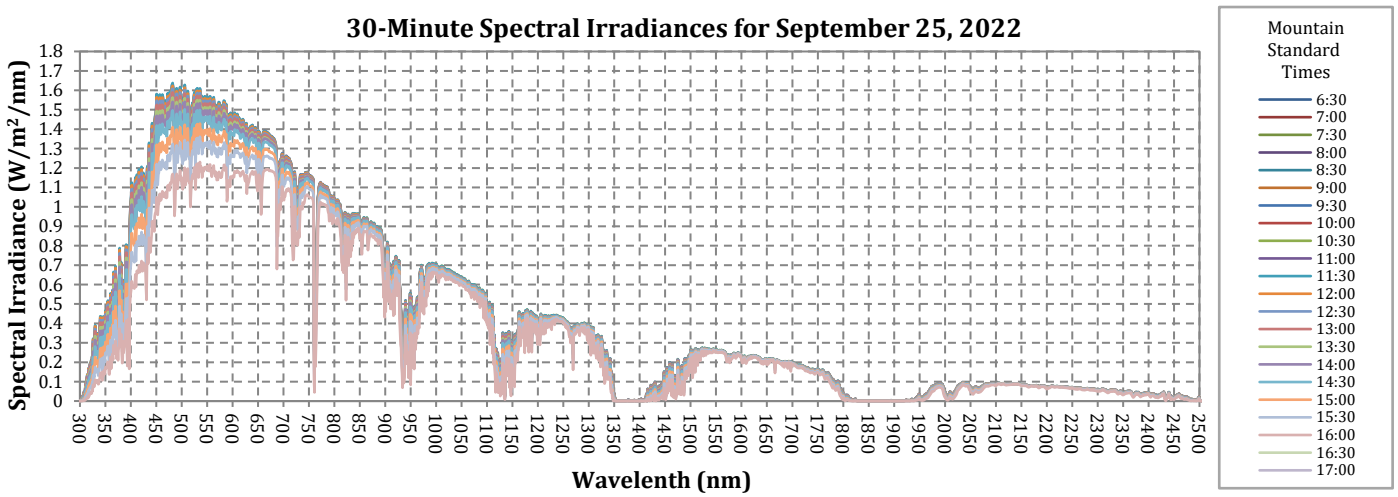

Figure B-7. 30-minute spectral irradiances for September 25, 2022

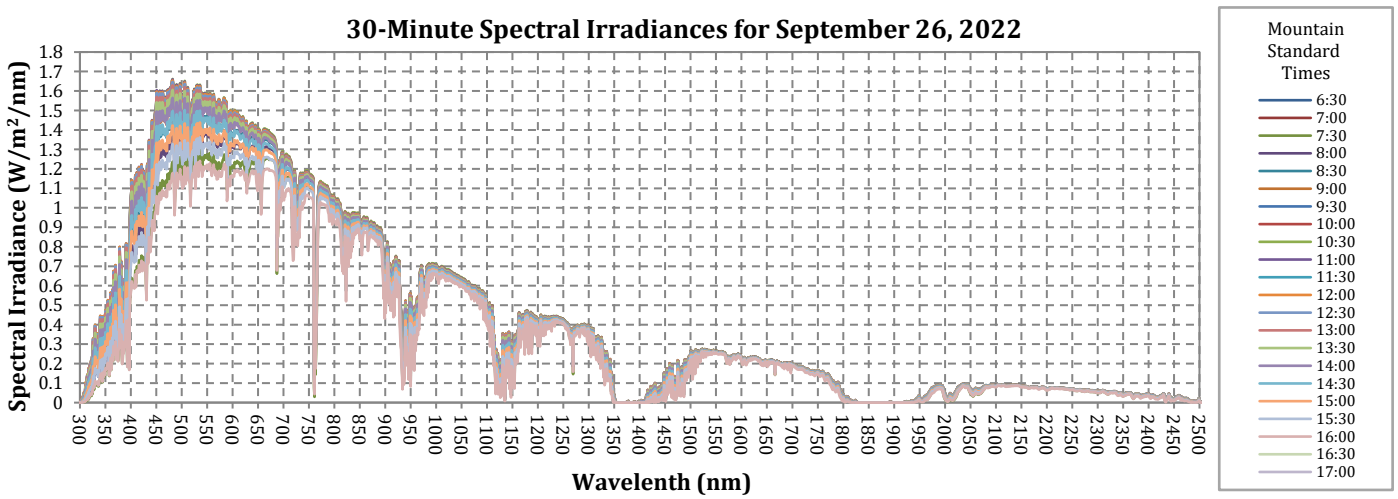

Figure B-8. 30-minute spectral irradiances for September 26, 2022

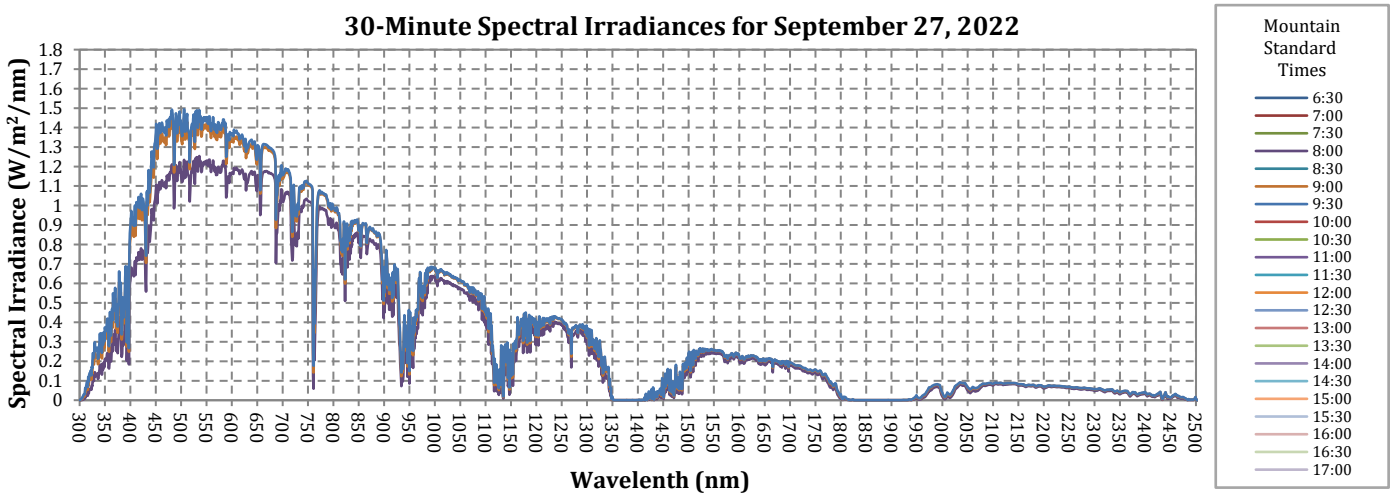

Figure B-9. 30-minute spectral irradiances for September 27, 2022

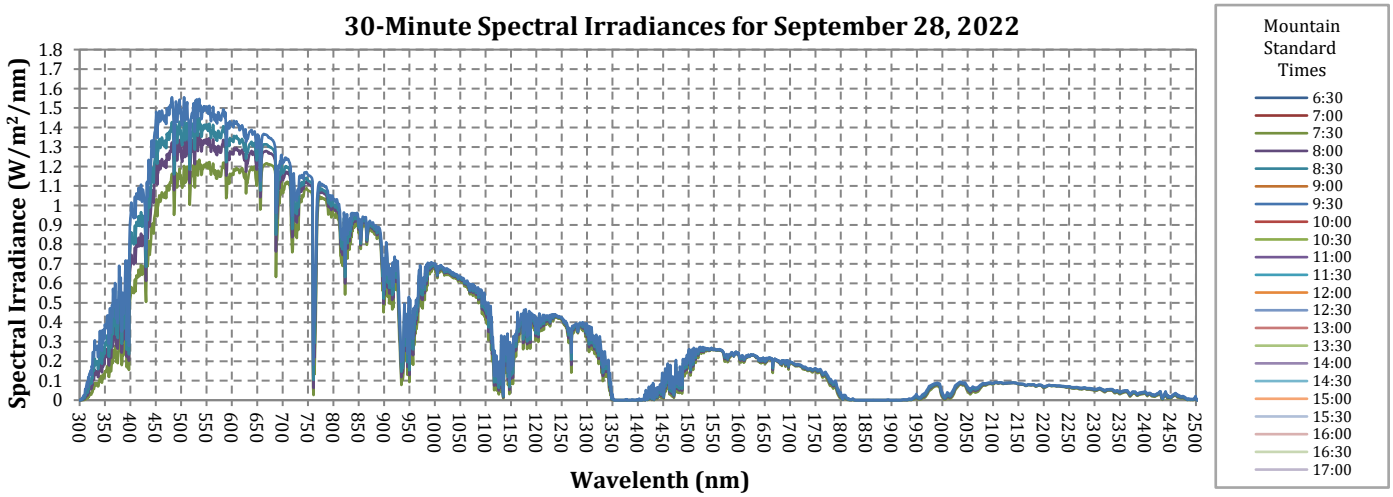

Figure B-10. 30-minute spectral irradiances for September 27, 2022

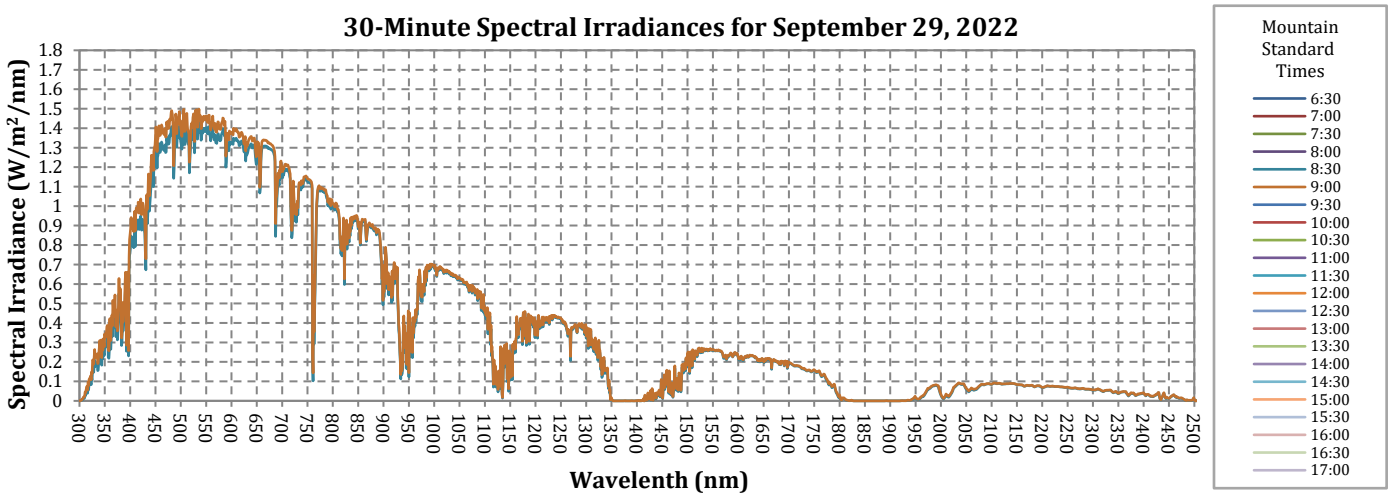

Figure B-11. 30-minute spectral irradiances for September 25, 2022

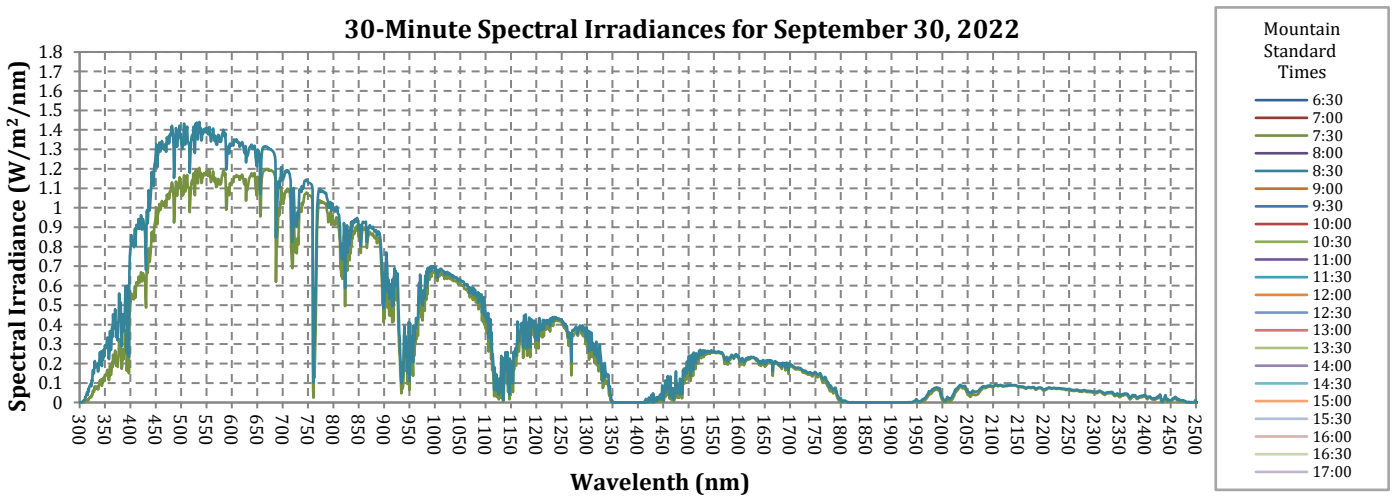

Figure B-12. 30-Minute Spectral Irradiances for September 27, 2022

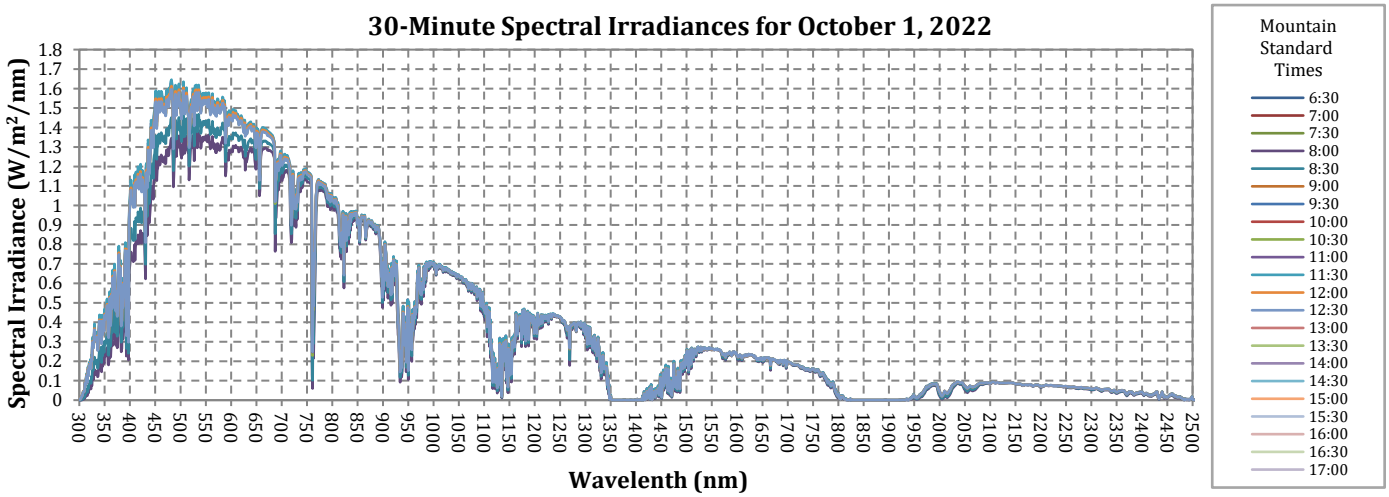

Figure B-13. 30-Minute Spectral Irradiances for October 1, 2022